Changes in SWEET-mediated sugar partitioning affect photosynthesis performance and plant response to drought

Emilie Aubry, Gilles Clement, Elodie Gilbault, Sylvie Dinant, Rozenn Le Hir

Changes in SWEET-mediated sugar partitioning affect photosynthesis performance and plant response to drought

Authors: Emilie Aubry[1], Gilles Clément[1], Elodie Gilbault[1], Sylvie Dinant[1] and Rozenn Le Hir[1,*]

Affiliations

[1]Université Paris-Saclay, INRAE, AgroParisTech, Institut Jean-Pierre Bourgin (IJPB), 78000, Versailles, France ; emilia.aubry@orange.fr (E.A.); gilles.clement@inrae.fr (G.C.); elodie.gilbault@inrae.fr (E.G.); sylvie.dinant@inrae.fr (S.D.); rozenn.le-hir@inrae.fr (R.L.H.)

Corresponding author: Dr R. Le Hir

Telephone: +33 1 30 83 36 56

Fax: +33 1 30 83 30 96

rozenn.le-hir@inrae.fr

ORCID ID : 0000-0001-6076-5863

Co-authors email addresses:

Emilie Aubry: emilia.aubry@orange.fr

Gilles Clément: gilles.clement@inrae.fr

Elodie Gilbault: elodie.gilbault@inrae.fr

Sylvie Dinant: sylvie.dinant@inrae.fr

Summary statement: Changes in intercellular and intracellular sugar transport mediated by SWEET11 and SWEET17 impact negatively or positively photosynthesis, respectively. In addition, a fine tuning of the expression of SWEET11, SWEET16 and SWEET17 is needed in Arabidopsis to properly respond to drought stress.

Abstract

Sugars, produced through photosynthesis, are at the core of all organic compounds synthesized and used for plant growth and response to the environmental changes. Therefore, their production, transport and utilization is highly regulated and integrated throughout the plant life cycle. The maintenance of sugar partitioning between the different subcellular compartments (e.g., cytosol, vacuole, chloroplast), and mediated by different families of sugar transporters (e.g., SUC/SUT, SWEET, ERDL), is instrumental to adjust the photosynthesis performance and response to abiotic constraints. Here we investigated in Arabidopsis the consequences of the disruption of four genes coding for SWEET sugar transporters (SWEET11, SWEET12, SWEET16 and SWEET17) on plant photosynthesis and response to drought. Our results show that, the disruption of the intercellular sugar transport, mediated by SWEET11, negatively impacts photosynthesis efficiency and net CO_2 assimilation while the stomatal conductance and transpiration are increased. These defects are accompanied by an impairment of both cytosolic and chloroplastic glycolysis leading to an accumulation of soluble sugars, starch and organic acids. Further, our results suggest that in the *swt11swt12* mutant, the sucrose-induced feedback mechanism on stomatal closure is poorly efficient. On the other hand, changes in fructose partitioning in mesophyll and vascular cells, mediated by SWEET17, positively impact photosynthesis probably through an increased starch synthesis together with a higher vacuolar sugar storage. Finally, our work shows that, a fine tuning, at transcriptional and/or translational levels, of the expression of SWEET11, SWEET16 and SWEET17 is needed in order to properly respond to drought stress.

Keywords: Photosynthesis, sugar transport, SWEET transporters, leaves, vascular system, drought stress

Introduction

Sugars are the cornerstone of plant growth, development and response to environmental changes. They are produced by photosynthesis and are then used as carbon skeletons for several anabolic reactions of both primary (e.g. starch and cellulose synthesis) and specialized metabolisms (Louveau and Osbourn 2019). In addition, they act as primary signals in transduction pathways and can serve as osmoprotectants and ROS scavengers in response to abiotic constraints (Saddhe et al. 2021). To achieve this wide range of functions, sugars should be transported from their synthesis site (i.e., photosynthetic source leaves) to their site of use (i.e., sink organs) through the combined action of plasmodesmata and a complex set of active and passive transporters such as sugar will eventually be exported transporters (SWEET) and sucrose transporters (SUC). At all time of the day, plants are constantly adjusting their production, transport and utilization (e.g., energy production, storage) of sugars to sustain an appropriate growth. Indeed, if sink organs are not active enough or if sugar loading in source leaves is impaired, sugars accumulate in source leaves and photosynthesis is inhibited. This phenomenon has been described as the metabolic feedback regulation of photosynthesis (Paul and Pellny 2003). On the other hand, an increased demand of sink organs can enhance photosynthesis (Ainsworth and Bush 2011). At the cell level, manipulations of the vacuole-cytosol sugar exchanges also modify the plant photosynthesis performance in a similar manner. For instance, photosynthesis is promoted in the absence of *PtaSUT4* coding for a tonoplastic sugar exporter or when *AtTST1*, responsible for loading sugars inside the vacuole, is overexpressed (Wingenter et al. 2010; Frost et al. 2012). It has been suggested that a decrease in the cytosolic sugar content is taking place in both cases. At the opposite, the suppression of the expression of *StTST3.1* a tonoplastic sugar importer, potentially leading to an increased cytosolic sugar content, negatively affects leaf photosynthesis in potato (Liu et al. 2023a). In the same line, the overexpression of the chloroplastic glucose facilitator pGlcT2 or the concurrent loss-of-function of pGlcT1 and maltose exporter MEX1, in which the cytosolic glucose availability is proposed to be increased, displays impaired photosynthetic properties (Cho et al. 2011; Valifard et al. 2023).

Due to the global climate change that earth is facing, recurring or prolonged periods of drought are taking place and are negatively affecting plant growth and yield along with its health and survival (Ghadirnezhad Shiade et al. 2023). When plants are facing drought stress several parallel mechanisms are taking place in the source leaves. The leaves first close its stomata to avoid losing more water by transpiration. This lowers the CO_2 absorption and therefore lower the photosynthesis which contributes to an increase in reactive oxygen species (ROS) production. To compensate the photosynthesis decrease, the source leaves breakdown their starch reserves to produce soluble sugars that will be both transported to sink organs such as roots in which they will be used for growth and they will be stored in the vacuole thereby maintaining osmotic potential and turgidity (Kaur et al. 2021). The soluble sugars produced will also be used as ROS scavengers to alleviate their negative effects (Keunen et al. 2013). Therefore, the transport of sugars between organs and subcellular compartments constitutes an important control point to ensure an appropriate answer of the plant to drought. Despite the high number of sugar transporters identified so far in plants, there is relatively few reports about their contribution to the plant response to drought stress (Kaur et al. 2021). Especially, it has

been shown that expression of members of the sucrose transporter (SUC/SUT) family could be up or downregulated in response to drought, depending on the phloem loading strategy (apoplasmic versus symplasmic loaders) (Xu et al. 2018). More precisely, in Arabidopsis, the expression of *SUC2*, coding for a sucrose transporter localized at the plasma membrane and responsible for phloem loading, and of *SUC4*, coding for a tonoplastic sucrose transporter, are upregulated in response to drought (Durand et al. 2016; Xu et al. 2018). In addition, the expression of several genes coding for members of the SWEET transporter family, namely *SWEET11*, *SWEET12*, *SWEET13* and *SWEET15*, is increasing in Arabidopsis leaves in response to water deficit (Durand et al. 2016). These results suggest that both improved phloem loading and tonoplastic sugar storage are required for plant response to water deprivation. It has been shown that several members of the early response to dehydration six-like (ERDL6) transporter family, which facilitate tonoplastic sugar transport, are also upregulated in response to water deprivation most probably in order to keep sugars inside the vacuole to maintain turgidity (Yamada et al. 2010; Slawinski et al. 2021). In the same line, we recently showed that in belowground organs, the expression of the gene coding for the fructose-specific SWEET17 transporter similarly as the genes coding for the tonoplastic sugar transporters TST1 and TST2 are transiently upregulated in response to a PEG-induced drought stress (Valifard et al. 2021). Logically, the *swt17* mutant displays a reduced tolerance to drought than the wild type when grown in soil (60% or 40% field capacity) (Valifard et al. 2021). On the other hand, the heterologous overexpression of apple *MdSWEET17* in tomato enhances drought tolerance (by water withholding for 15 days) via fructose accumulation (Lu et al. 2019). Finally, it was recently established that the phosphorylation of SWEET11 and SWEET12 by the SnRK2 kinase in leaves is required to regulate the plant root:shoot ratio under drought stress (by withholding water for 21-25 days), thereby promoting sucrose transport towards the roots (Chen et al. 2022). As a consequence, the double mutant *swt11swt12* has been shown to be less resistant to drought (Chen et al. 2022).

Altogether, these examples illustrate that both intercellular and intracellular sugar transport should be highly coordinated to achieve a proper photosynthesis in normal growth conditions but also to maintain growth in response to drought. However, previous reports only addressed the effects of either a disruption of plasma membrane sugar transporters or tonoplastic sugar transporters. In this work we propose to go a step further by exploring the simultaneous disruption of SWEET11 and SWEET12 transporters, which are involved in phloem loading (Chen et al. 2012), and of the tonoplastic SWEET16 and SWEET17 transporters controlling the cytosolic sugar availability, on the plant photosynthetic performance and response to drought stress.

Materials and Methods

Plant material and growth conditions

The following Arabidopsis lines have been used in this work: Columbia-0 accession (used as wild-type plants and hereafter referred as WT), the *sweet11-1sweet12-1* and the *sweet16-4sweet17-1* double mutant lines (hereafter referred as *swt11swt12* and *swt16swt17*, respectively) (Le Hir et al. 2015; Aubry et al. 2022) and the *sweet11-1sweet12-1sweet16-4sweet17-1* (hereafter referred as *swt-q*) (Hoffmann et al. 2022). To synchronize germination, seeds were stratified at 4°C for 72 hours in 0.1 % agar solution. Plants were grown in a growth chamber in short days (8 hours day/16 hours night and 150 µmol m^{-2} s^{-1}) at 21/19°C (day/night temperature)

with 65% relative humidity, for the thermal and PAM imaging, the gas exchanges measurements and the starch quantification. Alternatively, for the metabolomic analysis (under normal and drought conditions), the targeted gene expression analysis and histochemical analysis and fluorometric quantification of GUS activity, seeds were sown on peatmoss soil plugs in the *Phenoscope* phenotyping robot under short days (8 hours day/16 hours night and 230 µmol m^{-2} s^{-1}) at 21/17°C (day/night temperature) with 65% relative humidity as described in Tisné et al. (2013) under different water treatment. More precisely, seeds were let grown for 8 days with a soil water content (SWC) of 100 %. After 8 DAS (days after sowing), they are transferred to the phenotyping robot (the *Phenoscope*, https://phenoscope.versailles.inrae.fr/) and watering is maintained through individual pot weight at a specific SWC as described in Tisné et al. (2013). Three watering conditions were tested: '60% SWC' corresponds to 60% of the maximum SWC (representing 4.1g H2O per g of dry soil) as a well-watered control condition (stably reached and maintained from 12DAS), '30% SWC' (i.e. 30% of the maximum SWC: 1.6g H2O per g of dry soil) corresponding to a mild drought stress (stably reached and maintained from 16 DAS) and '25% SWC' (i.e. 25% of the maximum SWC: 1.1g H2O per g of dry soil) corresponding to a medium intensity drought stress (stably reached and maintained from 17 DAS). Plants were grown in these conditions until 31 DAS and entire rosettes are harvested at 31 DAS for the subsequent experiments. Thanks to daily pictures, the *Phenoscope* also gives access to cumulative growth parameters, such as Projected Rosette Area (PRA) as well as descriptive traits such as the rosette-encompassing convex hull (Convex Hull Area). Both parameters allow to calculate the rosette compactness (PRA/Convex Hull Area) which reflects the rosette morphology (Marchadier et al. 2019).

Pulse amplitude modulation (PAM) and thermal imaging

The chlorophyll fluorescence was measured using the IMAGING-PAM Maxi version (Heinz Walz GmbH, Effeltrich, Bayern, Germany) driven by the ImaginWin version 2.41a software and equipped with the measuring head consisted of LED-Array illumination unit IMAG-MAX/L and a CCD camera IMAG-MAX/K4 mounted on IMAG-MAX-GS stand. The plants were kept in the dark for a minimum of 20 min prior the measurements. The light curves were performed by exposing plant to different light intensities from 1 PAR (µmol photons m^{-2} s^{-1}) to 701 PAR. The complete rosette was included in the area of interest (AOI) and from the measured values, the derived Fv/Fm ratio, the effective quantum yield of PSII [Y(II)], the electron transport rate (ETR) and the quantum yield of non-photochemical quenching [Y(NPQ)] were calculated according to the equipment manual and represent the mean values of all pixels within an AOI.

Thermal images were obtained using a FLIR A320 infrared camera (Inframetrics, FLIR Systems, North Billerica, MA, USA) equipped with a 16 mm lens. Temperature resolution was below 0.1 °C at room temperature. Straight temperature images generated by the camera software on the basis of manufacturer calibration were used. Leaf emissivity was set to 0.970. The camera was mounted vertically at approximately 30 cm above the leaf canopy for observations, and was connected to a laptop equipped with the ThermaCAM Researcher Pro 2.9 software for pictures acquisition and analysis. On each plant, the total rosette was analysed and the minimum (Min), maximum (Max) and the difference maximum-minimum (Max-Min) temperature were given by the software.

Gas-exchange measurements

A LI-COR 6800F (LI-COR, Lincoln, NE, USA) infrared gas analyzer, equipped with a light source, was used for measuring the gas exchanges. Measurements were performed from 9:00 to 12:00. Leaves were clamped into a 2 cm^2 chamber. Irradiance level of light was set at 150 µmol photons m^{-2} s^{-1}. CO_2 concentration was set at 400 ppm at constant leaf temperature (around 27°C) and at constant vapor pressure deficit (VPD) (around 1.5 kPa). The net CO_2 assimilation (A_n), the stomatal conductance (g_{sw}), the intercellular CO_2 concentration (C_i) and the transpiration rate (E) were measured. The values of the water use efficiency (WUE) and of the intrinsic water use efficiency (WUEi) were then calculated as the A_n/E and A_n/g_{sw} ratio, respectively. Six plants per genotype were analyzed and on each plant, 2-3 leaves were measured.

Starch quantification

Starch was quantified from approximately 15-19 mg of whole rosette leaves grown for 43 days in short days and previously lyophilized. The samples were extracted by using an hydroalcoholic extraction consisting of a first step of Ethanol 80% at 90°C for 15 min, a second step of Ethanol 30% at 90°C for 15 min and a last step of water at 90°C for 15 min. Between each extraction round, a centrifugation step at 5 000 rpm for 3 min allow to collect the supernatants that could be used for soluble sugars quantification if needed. The pellet was then dried in a drying oven at 50°C for 3h. After hydrolysing starch pellet by using thermostable α-amylase and amyloglucosidase, glucose was quantified by enzymatic reaction as described in Bergmeyer and Bernt (1974).

Histochemical analysis and fluorometric quantification of GUS activity

The lines expressing pSWEET11:SWEET11-GUS or pSWEET12:SWEET12-GUS (Chen et al. 2012) and pSWEET16:SWEET16-GUS or pSWEET17:SWEET17-GUS (Guo et al. 2014) in Col-0 background were used to assess SWEET11, SWEET12, SWEET16 and SWEET17 expression pattern in response to different watering regimes (i.e., 60% SWC, 30 % SWC and 25 % SWC). The histochemical GUS staining was performed according to Sorin et al. (2005). Pictures were taken either using an Axio zoom V16 microscope equipped with a Plan-NEOFLUARZ 2.3x/0.57 FWD 10.6mm objective and the ZEN (blue edition) software package (Zeiss, https://www.zeiss.com/). The fluorometric quantification of GUS activity was performed as described in Sehki et al. (2023). Enzymatic activity was measured via the derived products generated from a 4-MUG substrate with a Fluoroskan Ascent II (Thermo Fisher Scientific). GUS activity is presented in an arbitrary unit as the ratio between fluorescence data par minute and protein concentration.

Metabolomic analysis

All steps were adapted from the original protocols detailed in Fiehn (2006, 2016) and Fiehn et al. (2008). The detailed protocol is available in Amiour et al. (2012). Briefly, 30 mg of ground frozen rosette leaves per genotype and condition were used for metabolome analysis by an Agilent 7890A gas chromatograph (GC) coupled to an Agilent 5977B mass spectrometer (MS). The column was an Rxi-5SilMS from Restek (30 m with 10 m Integra-Guard column). During the extraction phase, ribitol at a concentration of 4µg/ml was added to each sample to allow metabolites absolute quantification. Then, a response coefficient was determined for

4 ng each of a set of 103 metabolites, respectively to the same amount of ribitol. This factor was used to give an estimation of the absolute concentration of the metabolite in what we may call a "one point calibration". Standards were injected at the beginning and end of the analysis. Data were analyzed with AMDIS (http://chemdata.nist.gov/mass-spc/amdis/) and TargetLynx softwares (Waters Corp., Milford, MA, USA). For each genotype and condition, between 7-8 plants were analysed. The table containing the raw data of the metabolomic profiling is presented in Supplementary Table S1.

RNA isolation and cDNA synthesis

RNAs were prepared from whole rosette leaves subjected to different water regimes and grown in short day conditions as described above. Samples were frozen in liquid nitrogen before being ground with a mortar and pestle. Powders were stored at -80°C until use. Total RNA was extracted from frozen tissue using TRIzol reagent (Thermo Fisher Scientific, 15595-026, https://www.thermofisher.com) and treated with DNase I, RNase-free (Thermo Fisher Scientific, EN0521, https://www.thermofisher.com). cDNA was synthetized by reverse transcribing 1 µg of total RNA using RevertAid H minus reverse transcriptase (Thermo Fisher Scientific, EP0452, https://www.thermofisher.com) with 1 µl of oligo(dT)18 primer (100 pmoles) according to the manufacturer's instructions. The reaction was stopped by incubation at 70 °C for 10 min.

RT-qPCR experiment

Transcript levels were assessed for four independent biological replicates in assays with triplicate reaction mixtures by using specific primers either designed with the Primer3 software (http://bioinfo.ut.ee/primer3-0.4.0/primer3/) or taken from the literature (Supplementary Table S2). qPCR reactions were performed in a 96-well transparent plate on a Bio-Rad CFX96 Real-Time PCR machine (Bio-Rad) in 10 µl mixtures each containing 5 µl of Takyon™ ROX SYBR® MasterMix dTTP Blue (Eurogentec, UF-RSMT-B0710, https://www.eurogentec.com/), 0.3 µl forward and reverse primer (30 µM each), 2.2 µl sterile water and 2.5 µl of a 1/30 dilution of cDNA. The following qPCR program was applied: initial denaturation at 95°C for 5 min, followed by thirty-nine cycles of 95°C for 10 sec, 60°C for 20 sec, 72°C for 30 sec. Melting curves were derived after each amplification by increasing the temperature in 0.5°C increments from 65°C to 95°C. The Cq values for each sample were acquired using the Bio-Rad CFX Manager 3.0 software package. The specificity of amplification was assessed for each gene, using dissociation curve analysis, by the precision of a unique dissociation peak. If one of the Cq values differed from the other two replicates by > 0.5, it was removed from the analysis. The amplification efficiencies of each primer pair were calculated from a 10-fold serial dilution series of cDNA (Supplementary Table S1). Four genes were tested as potential reference genes: *APT1* (At1g27450), *TIP41* (At4g34270), *EF1α* (At5g60390) and *UBQ5* (At3g62250). The Normfinder algorithm (Andersen et al. 2004) was used to determine the gene most stably expressed among the different genotypes analyzed, namely *EF1α* in this study. The relative expression level for each genotype was calculated according to the ΔCt method using the following formula: average $E_t^{-Cq(\text{of target gene in A})}/E_r^{-Cq(\text{of reference gene in A})}$, where E_t is the amplification efficiency of the target gene primers, E_r is the reference gene primer efficiency, A represents one of the genotypes analyzed.

Statistical analysis

The statistical analyses were performed using either a student *t* test or a two-way ANOVA combined with a Tukey's comparison post-test, using R software. A *p*-value of < 0.05 was considered as significant. For the metabolome analysis, the Rflomics R package coupled with a shiny application and developed by INRAE was used and is available in GitLab (https://forgemia.inra.fr/flomics/rflomics). Briefly, the raw data were transformed using squareroot and a differential expression analysis was performed using the lmfit model of the limma package (Ritchie et al. 2015). The Rflomics package was also used to re-analyze the RNA-seq results obtained in Khan et al. (2023). Filtering and normalization strategies were performed as described in Lambert et al. (2020).

Results

Photosynthetic activity is impaired in swt11swt12 *double mutant*

It has been proposed for a long time that an excess sugars can trigger negative feedback regulation of leaf photosynthesis (Paul and Foyer 2001; Ainsworth and Bush 2011). In agreement with this, the disruption or overexpression of genes coding for sugar transporters, which potentially impact the cytosolic sugar availability, induce modifications of the photosynthetic performance (Wingenter et al. 2010; Frost et al. 2012; Khan et al. 2023; Liu et al. 2023b; Valifard et al. 2023). In an effort to gain more knowledge on the physiological consequences of impaired SWEET-mediated sugar transport, we measured chlorophyll fluorescence on the *swt11swt12*, *swt16swt17* and *swt-q* mutant lines along with the Col-0 wild-type (WT) plants. After 43 days of growth in growth chamber under short-days (SD) conditions, the projected rosette area (PRA) of both *swt11swt12* and *swt-q* mutant lines is smaller than that of the WT while no significant changes of the PRA of *swt16swt17* mutant is measured (Supplementary Fig. S1). Several parameters related to photosynthesis performance and nonphotochemical quenching using PAM imaging were measured. While the *swt16swt17* mutant did not shown any significant difference compared to the WT plants, we show that, along with an increase of the light intensity, the effective quantum yield of PSII photochemistry (Y(II)) is significantly lower in *swt11swt12* and *swt-q* mutants compared to WT plants (Fig. 1A). This is accompanied by a significant decrease of the electron transport rate (ETR) of both mutants compared to wild types (Fig. 1B). Moreover, we measured the fraction of energy dissipated in form of heat via the regulated non-photochemical quenching mechanisms [Y(NPQ)]. In wild-type plants, this fraction is logically increasing together with the increase of the light intensity (Fig. 1C). In both *swt11swt12* and *swt-q* mutants, the Y(NPQ) values are globally significantly higher compared to WT, showing that more energy is dissipated in form of heat in the mutant lines. Thus, avoiding PSII damage that could have occurred because of the impaired mutant capacity of efficiently using light. Altogether these results point to the fact that impairment of both *SWEET11* and *SWEET12* expression leads to impaired photosynthetic performance.

Gas-exchange parameters are altered in sweet *mutant lines*

Since feedback between CO_2 assimilation and photosynthetic activity has been shown, we further explored if this lower photosynthetic capacity could be linked to a limitation in the CO_2 assimilation. At the leaf level, the gas exchanges in the different mutant lines were thus assessed (Fig. 2A-F). Under ambient light conditions, the stomatal conductance (g_{sw}) along with the transpiration rate (E) of the *swt11swt12* mutant line tend to increase compared to WT plants (Fig. 2A-B). In the *swt-q* mutant line, both transpiration rate and stomatal conductance are significantly increased compared to wild-type plants (Fig. 2A-B). In addition, a tendency, albeit not significant, for a lower net CO_2 assimilation (A_{net}) was measured in both *swt11swt12* and *swt-q* lines (Fig. 2C). On the contrary, the assimilation rate as well as the stomatal conductance and the transpiration rate of the *swt16swt17* double mutant are significantly improved compared to WT (Fig. 2A-C). Further, we show that the intracellular CO_2 concentration (Ci) is significantly higher in all the *sweet* mutant lines compared to wild-type plants (Fig. 2D). This increase is logical since Ci calculation is more dependent from variations in g_{sw} and E than that of A_{net}, according to the equation of von Caemmerer and Farquhar (1981). Therefore, the improved A_{net} observed in *swt16swt17* is not important enough to induce a decrease in Ci values in this genotype. Nonetheless, this higher Ci suggests that more CO_2 substrate is available for assimilation in the *sweet* mutant lines. From these parameters the water-use efficiency (WUE), which represents the ratio of biomass produced per unit of water consumed (A/E ratio) and the intrinsic water-use efficiency (WUEi), which represents the ratio of net assimilation over the stomatal conductance (A/g_{sw} ratio), were calculated (Fig. 2E and F). Both *swt11swt12* and *swt-q* mutant lines display a reduced WUE and WUEi compared to wild type suggesting that less biomass is produced per unit of water loss (Fig. 2E and F). This is consistent with the smaller projected rosette area measured in both genotypes (Supplementary Fig. S1). On the other hand, the *swt16swt17* double mutant did not display any significant changes in WUE while the WUEi is significantly decreased compared to wild-type plants (Fig. 2E and F). These results suggest that the stomata functioning could be affected in these lines. By using thermal imaging, we were able to show that the maximum rosette temperature is significantly reduced in the *swt11swt12* double mutant and consequently the difference between the maximum and the minimum temperature is also significantly reduced in this line (Supplementary Fig. S2B-C). On the other hand, no significant change of these parameters is observed in both *swt16swt17* and *swt-q* mutants (Supplementary Fig. S2A-C). Altogether these results show that, in normal growth conditions, the impairment of the SWEET-mediated sugar transport impacts the equilibrium between CO_2 assimilation, transpiration and stomatal functioning.

SWEET transporters are differently expressed in rosette leaves

We exploited the published single-cell transcriptomics dataset of SD-grown leaves (Kim et al. 2021) to access the cell-specific expression of *SWEET11*, *SWEET12*, *SWEET16* and *SWEET17* (Supplementary Fig. S3). From this dataset we could see that *SWEET11* is mainly expressed in cluster of cells related to phloem parenchyma/procambium (cluster 10) and phloem parenchyma/xylem (cluster 18) (Supplementary Fig. S3A) while *SWEET12* is co-expressed with *SWEET11* in the phloem parenchyma/xylem cells (cluster 18) (Supplementary Fig. S3B). Surprisingly, *SWEET16* is almost exclusively expressed in the cluster 13 related to epidermal cells (Supplementary Fig. S3C) while an expression of *SWEET17* is found in nearly all the different

leaves cell types including the cluster 16 related to guard cells (Supplementary Fig. S3D). We completed these data by performing a histochemical analysis of GUS activity on lines expressing SWEET-GUS fusion proteins driven by their native promoter (Supplementary Fig. S3E-H). As expected from the single-cell transcriptomic analysis SWEET11 was expressed mainly in the leaves vascular system (Supplementary Fig. S3E). However, no expression of neither SWEET12 or SWEET16 was observed in our growing conditions (Supplementary Fig. S3F and G). Finally, SWEET17 expression was mainly observed in the vascular system of the leaves as well as in cells surrounding the vasculature (Supplementary Fig. S3H).

Sugars and organic acids of the TCA cycle are accumulating in sweet *mutants*

Next, the metabolic status of these lines was assessed by performing a global metabolomic profiling (Fig. 3 and Supplementary Table S1 for raw data) on plants grown in SD photoperiod on the *Phenoscope* to ensure high samples reproducibility. In *swt11swt12* and *swt-q* mutant lines, the global metabolites analysis identified 43 and 47 metabolites significantly different compared to wild-type plants, respectively (Supplementary Table S3). Consistently with previous reports (Chen et al. 2012; Le Hir et al. 2015), a significant accumulation of sucrose (fold-change (FC)=2.12), glucose (FC=1.81) and fructose (FC=1.61) was measured in the *swt11swt12* mutant (Fig. 3 and Supplementary Table S3). A significant increase of the same sugars is also measured in the *swt-q* mutants compared to WT (FC sucrose =1.87, FC glucose =1.68 and FC fructose =2.75). We also show that the fructose content is further increased in the quadruple mutant compared to the *swt11swt12* mutant (FC=1.69) (Fig. 3 and Supplementary Table S3). The content of other sugars including xylose, myo-inositol, melibiose, raffinose and mannose were also significantly accumulated in *swt11swt12* and/or *swt-q* mutants, albeit to a lower extent than sucrose, glucose and fructose (1.02<FC<1.20), while the content of stachyose was slightly decreased in these mutants (FC=0.96) (Fig. 3 and Supplementary Table S3). In addition, several organic acids among which almost all those involved in the TCA cycle (i.e., malate, citrate, succinate and 2-oxoglutarate) were significantly accumulated in both mutant lines (1.08<FC<2.04) (Fig. 3 and supplementary Table S3). On the other hand, the content of several amino acids (e.g., GABA, arginine, leucine, isoleucine, glycine) was slightly decreased only in the *swt-q* mutant line compared to wild-type plants (0.94<FC<0.98) (Fig. 3 and supplementary Table S3). In the *swt16swt17* mutant, the statistical analysis only identified fructose (FC=1.69) as differentially accumulated compared to wild-type plants (Fig. 3 and supplementary Table S3). To complete this metabolomic analysis, an analysis of the starch content of SD-grown leaves was performed and show that the three mutant lines are accumulating more starch than wild-type plants (Fig. 4).

sweet *mutants exhibit altered expression of genes related to sugar partitioning*

As stated above, *swt11swt12 and swt-q* mutants accumulate more soluble sugars and organic acids involved in the TCA cycle suggesting that the glycolysis may also be affected in these mutants. Indeed, the Krebs cycle is fuelled by pyruvate originating from cytosolic glycolysis performed during the day. On the other hand, the plastidial glycolysis allows the production of energy during the dark period. Thus, we checked, on the same samples than those used for the metabolite profiling, for alterations of the expression of genes

coding for the first steps of cytosolic and plastidial glycolysis (Table 1). We also measured the expression of genes involved in tonoplastic and plastidic sugar/triose phosphate transport to get a global picture of the metabolite's dynamic in the different subcellular compartments (Table 1).

During the day, sucrose synthesis in the cytosol in leaves is fueled mainly by triose phosphates exported from the chloroplasts by the TRIOSE-PHOSHATE/PHOSPHATE TRANSLOCATOR (TPT) and are first converted into fructose-1,6-biphosphate (Fru-1,6-P_2) by the FRUCTOSE BIPHOSPHATE ALDOLASE (FBA). Then the Fru-1,6-P_2 is dephosphorylated into fructose-6-phosphate (Fru-6-P) by FRUCTOSE 1,6-BIPHOSPHATASE (cyFBP/FINS1) or Fru-6-P is phosphorylated into Fru-1,6-P_2 by PHOSPHOFRUCTOKINASE (PFK). Moreover, the conversion of Fru1,6-P_2 into Fru-6-P is under the direct regulation of the fructose 2,6-biphosphate produced by the 6-PHOSPHOFRUCTO-2-KINASE/FRUCTOSE-2,6-BIPHOSPHATASE (F2KP) enzyme (McCormick and Kruger 2015). Therefore, the phosphorylation/dephosphorylation of the cytosolic fructose-6-P is critical for the balance between sucrose and starch production.

In *swt11swt12* mutant, we measured a significant upregulation of the *F2KP* and *PFK1* expression together with a global significant downregulation of the expression of genes coding for enzymes involved in converting triose phosphate into Fru-1,6-P_2 (i.e., *FBA4*, *FBA6*, *FBA7*) and for the triose-phosphate translocator (*TPT*) (Table 1). In addition, a significant decrease of the expression of *TONOPLAST SUGAR TRANSPORTER1* (*TST1*) coding for a glucose and fructose importer and an increase of the expression of *GLC6-PHOSPHATE TRANSLOCATOR2* (*GPT2*) are measured (Table 1). At the chloroplast level, we could measure a significant upregulation of several the genes related to the chloroplastic glycolysis (i.e., *pFBA3*, *PFK5*, *pPGI*). In agreement with previous report showing an accumulation of starch in this mutant grown under SD conditions (Gebauer et al. 2017), a significant upregulation of *ADG1* involved in starch biosynthesis is also shown (Table 1). In the *swt16swt17* mutant, we also measured a significant upregulation of both *F2KP* and *PFK1* expression (Table 1). However, depending on the isoforms, an up- or downregulation of *FBA* genes is observed (Table 1). At the chloroplast level, a significant upregulation of *HEXOKINASE3* (*HXK3*), *PHOSPHOGLUCO ISOMERASE1* (*pPGI*), *PFK5*, *pFBA1*, *pFBA2* and *pFBA3* along with *ADP GLUCOSE PYROPHOSPHORYLASE1* (*ADG1*) and *BETA-AMYLASE1* (*BAM1*), involved in starch biosynthesis and hydrolysis, is measured (Table 1). Finally, a significant overexpression of both *PLASTIDIC GLUCOSE TRANSLOCATOR* (*pGlcT)* coding for a chloroplastic glucose exporter and of *VACUOLAR GLUCOSE TRANSPORTER1* (*VGT1*) coding for a vacuolar glucose importer is observed (Table 1). In the quadruple mutant line, similar to both double mutant lines, a significant upregulation of the cytosolic isoform *PFK1* and the chloroplastic isoform *PFK5* is measured (Table 1). However, unlike both double mutants, the expression of *FBA7* (cytosolic isoform) is also significantly upregulated in the *swt-q* mutant (Table 1). In addition, *ADG1* and *GPT2* are also significantly upregulated in *swt-q* mutant as in *swt11swt12* mutant (Table 1). Finally, an upregulation of *MEX1* coding for a maltose transporter is only measured in the quadruple mutant (Table 1). Altogether these results show that, in addition to modifications of the photosynthesis, the partitioning of carbohydrates between sucrose and starch synthesis is strongly affected when the expression of *SWEET*

transporters is disrupted. Especially the increased expression of *F2KP*, *ADG, PFK5* and *GPT2* suggest that the sugar metabolism is redirected towards starch accumulation.

The rosette growth of swt-q *mutants is negatively affected in response to drought stress.*

Previously it has been shown that the *swt11swt12* double mutant is more susceptible to drought stress (Chen et al. 2022). Consistently we show that its WUE is significantly decreasing (Fig. 2). Alongside we also show that the *swt-q* mutant is also displaying a decreased WUE (Fig. 2). Therefore, we checked whether the *swt-q* mutant response to different drought scenario using the *Phenoscope* phenotyping robot. Three conditions were tested, non-limiting watering conditions (60% SWC), mild stress intensity (30% SWC) and medium stress intensity (25% SWC). The raw data are presented in Supplementary Table S4. When grown at 30% SWC, the projected rosette area (PRA) as well as the convex hull encompassing the rosette of wild type decreased compared to a SWC of 60% albeit not significantly (Fig. 5A-B). A further decrease of the SWC to reach 25% impacts significantly wild-type plants by reducing the PRA and the convex hull area by 35% and 50 %, respectively (Fig. 5A-B). Under normal watering condition, the PRA and the convex hull area of the *swt-q* mutant is significantly smaller than that of the wild type (Fig. 5A-B). Further, we show that the PRA and the convex hull area of the mutant line are more affected than the wild-type plants when grown under a mild-intensity stress (30 % SWC) (Fig. 5A-B). This increased sensitivity to drought is logical considering previous report showing that the *swt11swt12* double mutant is less resistant to drought stress when withholding water for 25 days (Chen et al. 2022). When grown under medium intensity stress (25 % SWC), the PRA and the convex hull area of the *swt-q* mutants are not significantly different from that of the wild-type plants grown in the same condition (Fig. 5A-B). Finally, we show that the PRA loss of WT plants is of 35% between both drought stress conditions (30 % SWC and 25 % SWC), while that of the *swt-q* mutant is reduced by 18% (Fig. 5A). Consistently, we observe for both traits a significant effect of the interaction between genotype and drought stress intensity (GxE) according to the result of a two-way ANOVA (Fig. 5A-B). We calculated the rosette compactness, which reflect the rosette morphology and potential default in leaves elongation, of both genotype under the different watering conditions (Fig. 5C). Interestingly the rosette of WT is significantly more compact when plants are subjected to a medium intensity stress (25 % SWC). On the other hand, under normal watering condition, the rosette of the *swt-q* mutant is smaller but also more compact than that of the wild type (Fig. 5C). However, unlike WT plants, the compactness of the *swt-q* rosette does not significantly change in response to drought stress (Fig. 5C). Overall, these results show that despite having a smaller and more compact rosette in normal watering conditions (60 % SWC) *swt-q* mutants display an increased sensitivity to drought.

Metabolic status of swt-q *mutant and wild-type plants under drought stress*

Next, we analysed the metabolites profiles of wild-type plants and *swt-q* mutant grown under the different watering regimes (Fig. 6 and supplementary Tables 4-8). As expected, mild and medium intensity stresses lead to changes in the metabolites content of the rosette of both genotypes (Supplementary Tables 5-9). In WT plants, only 3 metabolites were found to be accumulated in response to mild drought stress compared

to non-limiting watering conditions, namely ascorbate (FC=1.65), nicotinate (FC=1.008) and anhydroglucose (FC=1.11) (Fig. 6 and Supplementary Table S5). Ascorbate and nicotinate are both involved in oxidative stress and redox reactions while anhydroglucose results from the hydrolysis of cell wall compounds (Durand et al. 2019). On the other hand, the content of 51 metabolites over a total of 54 were differentially reduced in response to mild intensity stress (30% SWC) (Fig. 6 and Supplementary Table S5), among which 13 amino acids, 10 organic acids as well as sugars (e.g., fructose, trehalose) and phosphorylated sugars (e.g., glucose-6-phosphate, fructose-6-phosphate). In response to medium intensity drought stress (25% SWC), we identified 52 metabolites differentially altered in comparison with the non-limiting condition (60% SWC), among which 18 metabolites were accumulated and 34 were reduced (Supplementary Table S5). The content of proline tends to increase in response to medium drought stress albeit not significantly (Supplementary Fig. S4A). Nonetheless, we found a slight but significant accumulation of the 1-pyrroline-5-carboxylase (precursor of proline) (FC=1.014) along with an increased expression of the *DELTA 1-PYRROLINE-5-CARBOXYLATE SYNTHASE2* (*P5CS2*) gene responsible for the proline synthesis in response to both drought stress conditions (Supplementary Table S6 and Supplementary Fig. S4B). Several organic acids such as ascorbate and intermediate of the Krebs cycle (e.g., citrate, citramalate, fumarate, malate) were also accumulated (Fig. 5 and Supplementary Table S6) (1.02<FC<1.87). Finally, the content of several sugars, already known to be involved in the plant response to drought, were also increased but at a slight level (e.g., raffinose, myo-inositol, galactinol) (1.08<FC<1.19). Similarly, to the response to mild drought stress, the content of several amino acids along with sugars and sugar-phosphate were reduced in response to medium drought stress (Fig. 5 and supplementary Table S6). Since the most important effect of drought stress on WT rosette growth was observed in response to 25 % SWC (Fig. 5), we also identified metabolites specifically altered in response to medium drought stress. The content of 15 metabolites were specifically accumulated among which several organic acids (e.g., malate, fumarate, citrate, citramalate, galactonate, erythronate, 1-pyrroline-5-carboxylate) and sugars (e.g., raffinose, myo-inositol, xylitol) (Fig. 6 and Supplementary Fig. S5A). On the other hand, the content of only 5 metabolites were specifically decreasing in response to medium drought stress (i.e., putative hexose-P, C12:0 dodecanoate, galactosylglycerol, U2390.0/04 [1-Benzylglucopyranoside] and a breakdown product of glucosinolate) (Fig. 5 and Supplementary Fig. S5B).

In *swt-q* mutants, 22 and 20 metabolites were significantly accumulating when grown under mild drought stress (30 % SWC) or medium drought stress (25 % SWC) compared to non-limiting watering condition, respectively (Fig. 6 and Supplementary Tables S7-8). Nineteen of them were found common between mild and medium intensity drought stress (e.g., raffinose, sucrose, erythronate, 1-pyrroline-5-carboxylate, anhydroglucose, ribonate, malate, citramalate, myo-inositol, fumarate, nicotinate, ascorbate, galactinol and glucopyranose) (Supplementary Tables S7-8). Especially, fumarate was strongly accumulated in both stress conditions (FC=2.91 in 30 % SWC and FC=2.34 in 25 % SWC) (Supplementary Tables S7-8). Only fructose, putrescine and succinate were specifically accumulated in response to mild intensity drought stress (Fig. 6 and Supplementary Table S7-8). Finally, 47 and 45 metabolites were shown to have a decreased content in response to mild and medium drought stress, respectively (Supplementary Tables S7-8). Like for accumulating metabolites, most of the decreasing metabolites were common between both stress conditions

(Supplementary Fig. S5 and Supplementary Tables S7-8). Further we show that only proline was specifically accumulating in *swt-q* subjected to 25 % SWC (FC=1.13) (Supplementary Fig. S5C) while xylose, glycine, alpha-tocopherol, galactosylglycerol, a fatty acid methyl ester and an unknown metabolite related to ketohexose were specifically decreasing in response to 25 % SWC (Supplementary Fig. S5D).

Finally, we looked for metabolites responding to the interaction between genotype and environment. Eight metabolites (i.e., isoleucine, leucine, succinate, raffinose and sucrose, a-aminoadipate and melezitose) were shown to be significant to the combination of genotype and environment (60% SWC vs 30 % SWC) (Supplementary Table S9). Especially, unlike wild-type plants, *swt-q* mutants accumulate mainly sucrose in response to medium drought stress (FC=2.38) and a slight accumulation of raffinose (FC=1.15) and an unknown metabolite related to hexose-phosphate (FC=1.008) is also shown (Fig. 6 and Supplementary Table S9). On the other hand, isoleucine and leucine are slightly but significantly accumulating in wild-type plants unlike in *swt-q* mutants (FC=1.02) (Fig. 6 and Supplementary Table S9). When looking at the comparison between 60 % SWC and 25 % SWC, a specific accumulation of melibiose, sucrose, aconitate and melezitose is measured in *swt-q* mutants (Fig. 6 and Supplementary Table S9). On the other hand, while citrate significantly accumulates in WT in response to medium drought stress, its content (already high in normal conditions) did not change in *swt-q* mutant (Fig. 6 and Supplementary Table S9).

In response to drought stress, the genes involved in starch synthesis and degradation are upregulated in swt-q *mutants compared to WT plants*

We further analysed the *swt-q* mutant response to drought stress by quantifying the changes of expression of genes related to drought response, photosynthesis/respiration and those involved in sugar partitioning in the different watering conditions (Table 2). In response to drought stress, *swt-q* mutant responds similarly to WT plants by significantly upregulating the expression of *RESPONSE TO DESSICATION 29A* (*RD29a*), *P5CS2* and *EARLY RESPONSE TO DEHYDRATION SIX-LIKE1* (*ERDL3.07*/*ESL1*), known to be stress markers genes (Table 2). Despite an initial defect in photosynthesis performance (Fig. 1), the photosynthesis marker genes (i.e., *RBSC3B*, *LHCB1.1*/*CAB2* and *LHCB1.3*/*CAB1*) were not significantly regulated in response to drought in the *swt-q* mutant while a slightly significant upregulation of the expression of *RBSC3B* is measured in WT plants in response to mild intensity drought stress (Table 2). Interestingly, a significant increase of expression of *γCA1*, coding for a carbonic anhydrase involved in mitochondrial respiratory chain, is measured in *swt-q* mutants in response to medium drought stress while no significant change of the expression of both *γCA1* and *γCA2* is observed in WT (Table 2). Regarding the chloroplast functioning, only slight changes of the expression of *pPGI* and *PFK5* are observed in WT plants while in *swt-q* mutant a significant increase of the expression of *FRK3* is measured in response to drought (Table 2). In addition, both genotypes are significantly downregulating cytosolic isoforms of fructokinase (i.e., *FRK2* and *FRK7*) in response to drought while a significant upregulation of cytosolic phosphofructokinases is measured only in WT plants in response to mild intensity drought (i.e., *PFK1* and *PFK7*) (Table 2). Finally, a significant upregulation of genes coding for enzymes involved in starch synthesis and degradation (i.e., *APL3*, *APL4* and/or *BAM1*) is measured in both genotypes in response to drought (Table 2). According to the slightly

significant result of the GxE interaction this upregulation is further increased in *swt-q* mutant in response to medium intensity drought stress (Table 2). This is accompanied by a significant upregulation of the expression of the gene coding for *MEX1*, a maltose transporter in both genotype in response to drought. This upregulation is significantly more important in *swt-q* mutant compared to wild type, suggesting that in response to drought the quadruple *sweet* mutant potentially synthesizes and degrades more starch and export more maltose than WT plants (Table 2).

SWEET transporters are regulated by drought at both transcriptional and translational levels

We also checked for the regulation of SWEET genes and proteins under the same *Phenoscope* conditions that previously used. Both *SWEET11* and *SWEET12* expression is significantly downregulating in response to medium intensity drought (Fig. 6A-B). However, no transcriptional regulation of both *SWEET16* and *SWEET17* in response to drought stress has been measured (Fig. 7C-D). At the translational level, we were unable to detect expression of SWEET12 transporters even in normal growth condition which is consistent with the absence of GUS staining previously observed (Supplemental Fig. S3F and Fig. 7E). Finally, the expression of SWEET17 transporters is not modified while less SWEET11 transporter and more SWEET16 transporters are expressed upon drought treatment (Fig. 7E).

Discussion

As the mains forms of carbohydrates, the balance between soluble sugars and starch synthesis and utilization is crucial for plants to ensure an appropriate growth under both normal and challenging environmental conditions (Dong and Beckles 2019). This equilibrium is achieved by the combined action of intercellular and intracellular sugar transporters, among which the SWEET transporters family. In this work, we further explore the phenotype of the sugar-accumulating *swt11swt12*, *swt16swt17* and *swt-q* mutant lines (Chen et al. 2012; Gebauer et al. 2017; Aubry et al. 2022; Hoffmann et al. 2022) regarding their photosynthesis performance and response to drought stress since both could be impacted by sugars (Goldschmidt and Huber 1992; Saddhe et al. 2021).

In short-days photoperiod, the analysis of the SWEET11 and SWEET12 expression pattern in rosette leaves reveals that only SWEET11 seems to be expressed in these conditions (Supplementary Fig. S1). Therefore, the phenotypes observed in the *swt11swt12* double mutant could be mainly attributed to the activity of SWEET11 (as homodimer or heterodimer with other SWEET transporters yet to be identified). The *swt11swt12* mutant line displays a significant accumulation of soluble sugars (i.e., sucrose, glucose and fructose) and starch as already previously shown (Chen et al. 2012; Gebauer et al. 2017; Aubry et al. 2022; Hoffmann et al. 2022). Moreover, an increased loss of water per unit of biomass produced is observed in this mutant as indicated by the lower WUE and WUEi (dependent on stomata functioning), together with an increase transpiration and stomatal conductance. In addition, a lower rosette leaves temperature was measured, suggesting mor evapotranspiration (Supplementary Fig. S2) and thus sustaining the hypothesis that stomata opening/closure is impaired in the *swt11swt12* mutant compared to WT plants. Previous works point out that in most species, including Arabidopsis, stomatal closure is sucrose-induced (Lawson et al. 2014; Kottapalli et

al. 2018). In this line, it was proposed that when the rate of sucrose synthesis exceeds the rate of sucrose loading into the phloem, the extra sucrose is carried towards the stomata by the transpiration stream to stimulate stomatal closure via an hexokinase-dependent or independent mechanisms, preventing the loss of water and downregulating CO_2 assimilation (Kelly et al. 2013; Lima et al. 2018). The seminal analysis of the *swt11swt12* mutant show that both transporters are involved in phloem sugar loading in leaves leading to an accumulation of sugars at the leaf level (Chen et al. 2012). Furthermore our results, showing the significant upregulation of the sugar-induced *GPT2, PFK5, ADG1, pPGI* and *pFBA3* together with the significant downregulation of the sugar-repressed *TPT*, *TMT1*/*TST1* and *FBA7* (Table 1), favoured the hypothesis of an accumulation of cytosolic sugars in the *swt11swt12* mutant (Weise et al. 2019; Khan et al. 2023 and Supplementary Table S10). Therefore, in the double mutant line, mesophyll-produced sucrose is not properly loaded and accumulate in the cytosol of the phloem parenchyma cells but maybe also in that of the mesophyll cells located between the stomata and the phloem parenchyma cells (Fig. 8A-B). Further, we propose that in this mutant, the mechanisms allowing sucrose to reach back the stomata via the transpiration stream are impaired avoiding the sucrose-induced stomatal closure and yielding to lower WUE and WUEi (Fig. 8A-B). Consequently, since stomatal closure seems poorly efficient (higher transpiration and stomatal conductance), it could account for the higher intracellular CO_2 concentration (Ci) measured in the *swt11swt12* mutant line (Fig. 2D). Finally, the question, of whether impaired function of quinone acceptors (Q_A and Q_B), inactivation of the Mn_4Ca cluster or the production of reactive oxygen species are responsible for the increased photodamage of the PSII observed in this mutant, needs to be further explored. Nonetheless it could be hypothesized that, because of the negative regulation of the expression of Calvin cycle genes by sugar accumulation, a poor recycling of $NADP^+$ and excessive electron transfer could take place, leading to ROS production and thus impacting PSII efficiency (Couée et al. 2006). Altogether it could be proposed that the sugar exchanges between parenchyma cells and companion cells, mediated by SWEET11, is crucial in the regulation of stomata functioning and the overall leaf photosynthesis. Thus, reinforcing the link between phloem loading and its impact on stomatal closure. In addition, in the *swt11swt12* and *swt-q* mutants, the expression of several genes involved in both cytosolic and plastidial glycolysis are also deregulated, which ultimately impacts the TCA cycle functioning and leads to an increase of several organic acids content (e.g., malate, maleate, citrate, citramalate, 2-oxoglutarate, succinate, aconitate) as measured in the metabolomic analysis (Table 1, Fig. 3 and Fig. 8A, B and D). In complement to the ATP production during photosynthesis (through the chloroplastic electron transport chain including the PSII), the TCA cycle generates the reducing equivalents NADH and $FADH_2$, in the mitochondrial respiratory chain, that fuel ATP synthesis by oxidative phosphorylation (Braun 2020). In illuminated leaves it has been shown that the TCA cycle is mainly functioning in a noncyclic mode (Tcherkez et al. 2009). The carboxylic acid metabolism provides carbon skeletons for nitrogen assimilation and aspartate biosynthesis rather than to synthetise ATP. Interestingly, the content of several amino acids (e.g., aspartate, GABA, arginine, leucine, isoleucine, threonine, glycine) is slightly impaired in both *swt11swt12* and *swt-q* mutants (Fig. 3). Our results concur to propose that in these mutant lines, the balance between ATP production (both from chloroplasts due to the impaired PSII efficiency and mitochondria) and N metabolism is modified most probably at the expense of ATP since aspartate is slightly accumulating in *swt11swt12* mutant (Fig. 3). In addition, it has been shown

that changes in malate/fumarate content in illuminated leaves may affect stomata functioning (Zhang and Fernie 2018). Indeed, after being produced by the TCA cycle, malate and fumarate are stored in the vacuole of the mesophyll cells. Then, by an unknown mechanism, their levels are altered in subsidiary cells which will lead to a high malate content in the guard cells that participate to the stomata closing (Lee et al. 2008; Zhang and Fernie 2018). In this work, the high malate content in leaves is associated with higher transpiration rate and stomatal conductance in *swt11swt12* and *swt-q* mutant lines suggesting that at least malate export from the vacuole is impaired in both mutants, thus providing another explanation for the defect in stomatal functioning (Fig. 8B and D).

In addition to the involvement of SWEET11 in the photosynthesis performance, our results show also that vacuole-cytosol sugar exchanges are crucial for this process (Fig. 8A and C). Especially, we show that SWEET17 is expressed mainly in the vascular system and the mesophyll cells (Supplementary Fig. S3) while SWEET16 seems to be completely absent from the whole rosette, suggesting that the phenotypes observed in the *swt16swt17* mutant are more likely dependent on the activity of the fructose-specific SWEET17 transporter. Unlike in *swt11swt12* and *swt-q* mutants, several gas exchanges-related parameters are higher in the *swt16swt17* mutant (i.e., net CO_2 assimilation, transpiration rate, stomatal conductance and Ci). However, the *swt16swt17* mutant transpires more than it assimilates CO_2 since the WUEi is significantly decreased while WUE is not statistically different from WT plants (Fig. 2). Unlike WUE, which has been shown in Arabidopsis to be positively linked to biomass accumulation, WUEi is more dependent on stomata (e.g. anatomy, physiology, leaf biochemistry and Calvin cycle activity) (Vialet-Chabrand et al. 2016; Bhaskara et al. 2022). In agreement, we did not observe any significant changes in biomass accumulation in this mutant line (Supplementary Fig. S1). Therefore, the significant changes in WUEi points to a defect related to the stomatal conductance. Among the factors influencing the WUEi, it has been shown that stomata size/density, opening/closure and changes in the leaf hydraulic conductance could affect stomatal and mesophyll conductance and therefore WUEi (Petrík et al. 2023). In the case of *swt16swt17*, it is unlikely that stomata closure/opening is affected since no change in the whole rosette temperature was measured in the *swt16swt17* (Supplementary Fig. S2 and Fig. 8C). However, even if we cannot exclude a defect in stomatal size and density in this mutant, we suggest that leaf cell wall defects could explain this lower WUEi. Indeed, we previously showed that xylem cell wall composition is altered in the stem of the *swt16swt17* mutant (Aubry et al. 2022). If cell wall defects (e.g., cell wall thickness, changes in hemicellulose/pectins ratio) are also present in leaves, it could therefore account for impaired leaf hydraulic conductivity and therefore stomatal/mesophyll conductance (Petrík et al. 2023). Interestingly, these changes in gas exchanges are accompanied with a specific increase of fructose content in the mutant rosette (Fig. 3). Until now it has been suggested that, in the *swt16swt17* mutant, the tonoplastic fructose content is likely enhanced at the expense of the cytosolic fructose content (Valifard et al. 2021; Aubry et al. 2022). Consistently, the expression of *pFBA1*, *pFBA2*, *FBA5*, *BAM1*, *pGlcT*, *PFK1* and *F2KP* is downregulated in the mutant line while their expression are upregulated in presence of high cytosolic fructose content induced in fructose-incubated leaf discs (Supplementary Table S7 and Khan et al. 2023). However, while the expression of the plastidial isoforms of *ADG1*, *pFBA3*, *PFK5* and *pPGI* is upregulated when cytosolic fructose content is high, their expressions are also upregulated in the *swt16swt17*

mutant line (Table 1 and Supplementary Table S10). From these, we postulate that fructose partitioning in the double mutant might be more complex than just an increased vacuolar fructose sequestration and that the plastidial and/or cytosolic fructose content could also be modified. Consequently, the modified fructose partitioning within the mesophyll cells and the vascular system positively impact the plant photosynthesis (Fig. 8C). One possible explanation for this could reside in the improved starch synthesis measured in the *swt16swt17* mutant (Table 1 and Fig. 4). Indeed, the expression of *pFBA1-3* genes which are part of the regeneration phase of the Calvin-Benson cycle and have been suggested to be important for starch synthesis (Lu et al. 2012) along with the expression of the *pPGI*, which is involved in starch biosynthesis during the light period (Preiser et al. 2020) and, the expression of *ADG1*, involved in starch synthesis, are significantly upregulated (Table 1). Moreover, despite the slight upregulation of *BAM1* expression together with *pGlcT* shown to export glucose after starch degradation (Cho et al. 2011), an increased starch content is measured in this line (Fig. 4). Since a correlation between high photosynthesis and up-regulation of starch metabolism genes have been shown (MacNeill et al. 2017) and that strong links between fructose and starch synthesis are established (e.g., FINS/FBP, F2KP) (Cho and Yoo 2011; McCormick and Kruger 2015), the increase starch accumulation could also account for the improved photosynthesis in the *swt16swt17* mutant (Fig. 8C).

It is well known that sugars, through their accumulation, are key compounds which affect plant tolerance to abiotic stresses. Especially, it has been proposed that an accumulation of sugars protect the plants against abiotic constraints due their role of osmolytes as well as ROS scavengers (Keunen et al. 2013; Saddhe et al. 2021). However, in response to drought, both Arabidopsis *swt11swt12* and *swt17* mutant lines, which accumulates sugars (most probably through an increase sugar export or an increase vacuolar sugar sequestration, respectively), have been shown to be more sensitive to drought stress imposed through PEG induction or through a decreased soil water content by water withholding (Valifard et al. 2021; Chen et al. 2022). On the other hand, the overexpression of the tonoplastic MdSWEET17 in tomato leads to an accumulation of sugars (most probably through an increase export of sugar to the cytosol) and an improved response to drought in tomato (Lu et al. 2019). These works suggest, therefore, that the response to drought is not just link to a global increase of sugar content in leaves but could be highly dependent on the sugar partitioning between vacuole and cytosol. Our results show that the *swt-q* mutant, in which sugar partitioning is altered, is more sensitive to drought even when imposed at a mild intensity (30 % SWC) (Fig. 5) and support therefore this hypothesis. The fact that in response to 25 % SWC, the PRA of *swt-q* mutant is not further decreased, could only reflect the fact that the PRA loss reached the maximum already at 30 % SWC. Besides impacting the plant morphology, drought stress also modifies plant physiology, among which a lower photosynthesis as a consequence of stomata closure (Kaur et al. 2021). Moreover an improved intrinsic water used efficiency (WUEi) is often associated with drought tolerance (Zargar et al. 2017). In normal watering conditions, like the *sw11swt12* mutant, the *swt-q* mutant displays a significant decrease of both WUE and WUEi (Fig. 1, Fig. 8D), thus accounting for the increased drought sensitivity of this mutant.

Despite this impaired photosynthesis performance (altered PSII efficiency and net CO_2 assimilation) (Fig. 8D), the photosynthesis does not seem to be further affected by drought in *swt-q* mutant compared to WT, since no change in the expression of photosynthesis marker genes is measured (Table 2). Nonetheless,

the *swt-q* mutant accumulates significantly more of both sucrose and glucose when exposed to drought (Fig. 5). In addition, the expression of genes involved in starch synthesis and degradation (i.e., *APL3*, *APL4*, *BAM1* and *MEX1*) is further upregulated in *swt-q* mutant compared to WT subjected to drought (Table 2). Interestingly, the stable expression of the sugar-repressed *LHCB1.3*/*CAB1* and sugar-induced *GPT2,* under drought, suggest that the cytosolic sugar level in *swt-q* mutant is not further modified in response to drought. This suggest that both glucose and sucrose could be stored in the vacuole, despite the disruption of *SWEET16* and *SWEET17*. This would require the use of another tonoplastic sugar facilitator such as ERDL3.07/ESL1, already known to be involved drought response (Yamada et al. 2010; Slawinski et al. 2021). Interestingly, the expression of *ERDL3.07/ESL1* is indeed significantly upregulated in *swt-q* in response to drought and could be responsible for loading vacuole with sugars to maintain the adequate balance between the different subcellular sugar pools. Consistently with an important role of the vacuole in plant drought response, we also identified that, in a wild type context, SWEET16 protein accumulation is positively regulated in response to drought (Fig. 7), most likely enhancing vacuolar sugar filling to maintain proper cell turgidity as proposed earlier (Xu et al. 2018; Kaur et al. 2021). In the literature, it has also been shown that, in LD-grown plants subjected to water stress, transcripts of the sugar transporters from the SUC/SUT and SWEET families are usually upregulated which will increase phloem loading and subsequently improved the water uptake by the xylem (Durand et al. 2016; Xu et al. 2018; Stanfield and Bartlett 2022). Alternatively, it has been shown that phloem loading is dynamically responding to the sucrose levels in the phloem through the regulation of the proton-coupled sucrose symporter by the sucrose levels in the leaf (Chiou and Bush 1998). Obviously, plants are tightly regulating their sugar phloem loading to adjust the phloem turgor pressure in response to water shortage. In line with this assumption, we show that in SD-grown plants, SWEET11 is repressed at both transcriptional and translational levels suggesting that sugar phloem loading in leaves is potentially decreasing in response to drought. Our results nicely complete the findings of Chen and colleagues (2022) who proposed that phosphorylation of both SWEET11 and SWEET12 in leaves is needed to promote sucrose transport towards root system and improved drought resistance. Therefore, SWEET11 expression is controlled at least at three different levels (i.e., transcriptional, translational and post-translational) allowing the plant to finely and constantly tune the sugar phloem loading to ensure a proper plant growth upon drought. Altogether, our results shed the light on the complementarity of SWEET11 and SWEET16 in balancing the intracellular and intercellular sugar content in order to properly respond to drought.

Conclusion

It has been long proposed that changes in sugar partitioning impact plant photosynthesis performance. Nonetheless, the molecular actors involved in such phenomenon are not well characterized. In this work, we propose that the intercellular sugar exchanges mediated by SWEET11 negatively impact photosynthesis while the intracellular fructose exchange mediated by SWEET17 leads to an improved photosynthesis. Furthermore, this work suggests that this impaired photosynthesis capacity is linked to several mechanisms such as an altered sucrose-induced feedback mechanism on stomatal closure or an improved starch accumulation between or within mesophyll and vascular system cells (including phloem parenchyma cells). This impaired sugar

partitioning and photosynthesis are associated with an enhanced sensitivity upon drought. Finally, we proposed that further attention should be paid on SWEET11 and SWEET16, expression of which is controlled at transcriptional and/or translational levels, in order to develop adequate strategies for improving plant response to drought.

Author Contributions

Conceptualization, R.L.H.; investigation, E.A., G.C. and R.L.H.; methodology, E.A., G.C., E.G., and R.L.H.; visualization, R.L.H.; writing—original draft, R.L.H.; writing—review and editing, S.D. and R.L.H.

Acknowledgments

We thank Olivier Loudet (head of the *Phenoscope* platform) for his help regarding the validation of the results coming from the *Phenoscope* experiments.

Data availability

The data supporting the findings of this study are available from the corresponding author, Rozenn Le Hir, upon request.

Conflicts of interest

The authors declare that the research was conducted in the absence of any commercial or financial relationships that could be construed as a potential conflict of interest.

Funding

This work has benefited from the support of IJPB's Plant Observatory technological platforms and from a French State grant (Saclay Plant Sciences, reference ANR-17-EUR-0007, EUR SPS-GSR) managed by the French National Research Agency under an Investments for the Future program (reference ANR-11-IDEX-0003-02) through PhD funding to E.A.

References

Ainsworth EA, Bush DR (2011) Carbohydrate export from the leaf: A highly regulated process and target to enhance photosynthesis and productivity. Plant Physiol 155: 64–69

Amiour N, Imbaud S, Clément G, Agier N, Zivy M, Valot B, Balliau T, Armengaud P, Quilleré I, Cañas R, Tercet-Laforgue T, Hirel B (2012) The use of metabolomics integrated with transcriptomic and proteomic studies for identifying key steps involved in the control of nitrogen metabolism in crops such as maize. J Exp Bot 63: 5017–5033

Andersen CL, Jensen JL, Ørntoft TF (2004) Normalization of real-time quantitative reverse transcription-PCR data: A model-based variance estimation approach to identify genes suited for normalization, applied to bladder and colon cancer data sets. Cancer Res 64: 5245–5250

Aubry E, Hoffmann B, Vilaine F, Gilard F, Klemens PAW, Guérard F, Gakière B, Neuhaus HE, Bellini C, Dinant S, Le Hir R (2022) A vacuolar hexose transport is required for xylem development in the inflorescence stem. Plant Physiol 188: 1229–1247

Bergmeyer HV, Bernt E (1974) Sucrose. In: Bergmeyer HV (ed) Methods of enzymatic analysis. Academic Press, New York, pp. 1176–1179

Bhaskara GB, Lasky JR, Razzaque S, Zhang L, Haque T, Bonnette JE, Civelek GZ, Verslues PE, Juenger TE (2022) Natural variation identifies new effectors of water-use efficiency in Arabidopsis. Proc Natl Acad Sci 119: e2205305119

Braun HP (2020) The Oxidative Phosphorylation system of the mitochondria in plants. Mitochondrion 53: 66–75

von Caemmerer S, Farquhar GD (1981) Some relationships between the biochemistry of photosynthesis and the gas exchange of leaves. Planta 153: 376–387

Chen L-Q, Qu X-Q, Hou B-H, Sosso D, Osorio S, Fernie AR, Frommer WB (2012) Sucrose efflux mediated by SWEET proteins as a key step for phloem transport. Science 335: 207–211

Chen Q, Hu T, Li X, Song CP, Zhu JK, Chen L, Zhao Y (2022) Phosphorylation of SWEET sucrose transporters regulates plant root:shoot ratio under drought. Nat Plants 8: 68–77

Chiou TJ, Bush DR (1998) Sucrose is a signal molecule in assimilate partitioning. Proc Natl Acad Sci U S A 95: 4784–4788

Cho M-H, Lim H, Shin DH, Jeon J-S, Bhoo SH, Park Y-I, Hahn T-R (2011) Role of the plastidic glucose translocator in the export of starch degradation products from the chloroplasts in Arabidopsis thaliana. New Phytol 190: 101–112

Cho YH, Yoo SD (2011) Signaling role of fructose mediated by FINS1/FBP in Arabidopsis thaliana. PLoS Genet 7: 1–10

Couée I, Sulmon C, Gouesbet G, El Amrani A (2006) Involvement of soluble sugars in reactive oxygen species balance and responses to oxidative stress in plants. J Exp Bot 57: 449–459

Dong S, Beckles DM (2019) Dynamic changes in the starch-sugar interconversion within plant source and sink tissues promote a better abiotic stress response. J Plant Physiol 234–235: 80–93

Durand M, Porcheron B, Hennion N, Maurousset L, Lemoine R, Pourtau N (2016) Water deficit enhances C export to the roots in A. thaliana plants with contribution of sucrose transporters in both shoot and roots. Plant Physiol 170: pp.01926.2015-p.01926.2015

Durand TC, Cueff G, Godin B, Valot B, Clément G, Gaude T, Rajjou L (2019) Combined proteomic and metabolomic profiling of the Arabidopsis thaliana vps29 mutant reveals pleiotropic functions of the retromer in seed development. Int J Mol Sci 20: 1–22

Fiehn O (2006) Metabolite profiling in Arabidopsis. Methods Mol Biol Clifton NJ 323: 439–447

Fiehn O (2016) Metabolomics by Gas Chromatography-Mass Spectrometry: Combined Targeted and Untargeted Profiling. Curr Protoc Mol Biol 114: 30.4.1-30.4.32

Fiehn O, Wohlgemuth G, Scholz M, Kind T, Lee DY, Lu Y, Moon S, Nikolau B (2008) Quality control for plant metabolomics: reporting MSI-compliant studies. Plant J Cell Mol Biol 53: 691–704

Frost CJ, Nyamdari B, Tsai C-J, Harding SA (2012) The Tonoplast-Localized Sucrose Transporter in Populus (PtaSUT4) Regulates Whole-Plant Water Relations, Responses to Water Stress, and Photosynthesis. PLOS ONE 7: e44467

Gebauer P, Korn M, Engelsdorf T, Sonnewald U, Koch C, Voll LM (2017) Sugar Accumulation in Leaves of Arabidopsis sweet11/sweet12 Double Mutants Enhances Priming of the Salicylic Acid-Mediated Defense Response. Front Plant Sci 8: 1–13

Ghadirnezhad Shiade SR, Fathi A, Taghavi Ghasemkheili F, Amiri E, Pessarakli M (2023) Plants' responses under drought stress conditions: Effects of strategic management approaches—a review. J Plant Nutr 46: 2198–2230

Goldschmidt EE, Huber SC (1992) Regulation of photosynthesis by end-product accumulation in leaves of plants storing starch, sucrose, and hexose sugars. Plant Physiol 99: 1443–1448

Guo W-J, Nagy R, Chen H-Y, Pfrunder S, Yu Y-C, Santelia D, Frommer WB, Martinoia E (2014) SWEET17, a facilitative transporter, mediates fructose transport across the tonoplast of Arabidopsis roots and leaves. Plant Physiol 164: 777–789

Le Hir R, Spinner L, Klemens PAW, Chakraborti D, De Marco F, Vilaine F, Wolff N, Lemoine R, Porcheron B, Géry C, Téoulé E, Chabout S, Mouille G, Neuhaus HE, Dinant S, Bellini C (2015) Disruption of the sugar transporters AtSWEET11 and AtSWEET12 affects vascular development and freezing tolerance in Arabidopsis. Mol Plant 8: 1687–1690

Hoffmann B, Aubry E, Marmagne A, Dinant S, Chardon F, Le Hir R (2022) Impairment of sugar transport in the vascular system acts on nitrogen remobilization and nitrogen use efficiency in Arabidopsis. Physiol Plant 174: e13830

van Hooren M, van Wijk R, Vaseva II, Van Der Straeten D, Haring M, Munnik T (2023) Ectopic Expression of Distinct PLC Genes Identifies 'Compactness' as a Possible Architectural Shoot Strategy to Cope with Drought Stress. Plant Cell Physiol pcad123

Kaur H, Manna M, Thakur T, Gautam V, Salvi P (2021) Imperative role of sugar signaling and transport during drought stress responses in plants. Physiol Plant 171: 833–848

Kelly G, Moshelion M, David-Schwartz R, Halperin O, Wallach R, Attia Z, Belausov E, Granot D (2013) Hexokinase mediates stomatal closure. Plant J 75: 977–988

Keunen E, Peshev D, Vangronsveld J, Van Den Ende W, Cuypers A (2013) Plant sugars are crucial players in the oxidative challenge during abiotic stress: Extending the traditional concept. Plant Cell Environ 36: 1242–1255

Khan A, Cheng J, Kitashova A, Fürtauer L, Nägele T, Picco C, Scholz-Starke J, Keller I, Neuhaus HE, Pommerrenig B (2023) Vacuolar sugar transporter EARLY RESPONSE TO DEHYDRATION6-LIKE4 affects fructose signaling and plant growth. Plant Physiol doi.org/10.1093/plphys/kiad403

Kim J-Y, Symeonidi E, Pang TY, Denyer T, Weidauer D, Bezrutczyk M, Miras M, Zöllner N, Hartwig T, Wudick MM, Lercher M, Chen L-Q, Timmermans MCP, Frommer WB (2021) Distinct identities of leaf phloem cells revealed by single cell transcriptomics. Plant Cell 33: 511–530

Kottapalli J, David-Schwartz R, Khamaisi B, Brandsma D, Lugassi N, Egbaria A, Kelly G, Granot D (2018) Sucrose-induced stomatal closure is conserved across evolution. PLOS ONE 13: e0205359

Lambert I, Paysant-Le Roux C, Colella S, Martin-Magniette M-L (2020) DiCoExpress: a tool to process multifactorial RNAseq experiments from quality controls to co-expression analysis through differential analysis based on contrasts inside GLM models. Plant Methods 16: 68

Lawson T, Simkin AJ, Kelly G, Granot D (2014) Mesophyll photosynthesis and guard cell metabolism impacts on stomatal behaviour. New Phytol 203: 1064–1081

Lee M, Choi Y, Burla B, Kim Y-Y, Jeon B, Maeshima M, Yoo J-Y, Martinoia E, Lee Y (2008) The ABC transporter AtABCB14 is a malate importer and modulates stomatal response to CO2. Nat Cell Biol 10: 1217–1223

Lima VF, Medeiros DB, Dos Anjos L, Gago J, Fernie AR, Daloso DM (2018) Toward multifaceted roles of sucrose in the regulation of stomatal movement. Plant Signal Behav 13: e1494468

Liu T, Kawochar MA, Liu S, Cheng Y, Begum S, Wang E, Zhou T, Liu T, Cai X, Song B (2023a) Suppression of the tonoplast sugar transporter, StTST3.1, affects transitory starch turnover and plant growth in potato. Plant J 113: 342–356

Liu T, Kawochar MA, Liu S, Cheng Y, Begum S, Wang E, Zhou T, Liu T, Cai X, Song B (2023b) Suppression of the tonoplast sugar transporter, StTST3.1, affects transitory starch turnover and plant growth in potato. Plant J 113: 342–356

Louveau T, Osbourn A (2019) The Sweet Side of Plant-Specialized Metabolism. Cold Spring Harb Perspect Biol 11: a034744

Lu J, Sun M hong, Ma Q jun, Kang H, Liu Y jing, Hao Y jin, You C xiang (2019) MdSWEET17, a sugar transporter in apple, enhances drought tolerance in tomato. J Integr Agric 18: 2041–2051

Lu W, Tang X, Huo Y, Xu R, Qi S, Huang J, Zheng C, Wu C (2012) Identification and characterization of fructose 1,6-bisphosphate aldolase genes in Arabidopsis reveal a gene family with diverse responses to abiotic stresses. Gene 503: 65–74

MacNeill GJ, Mehrpouyan S, Minow MAA, Patterson JA, Tetlow IJ, Emes MJ (2017) Starch as a source, starch as a sink: the bifunctional role of starch in carbon allocation. J Exp Bot 68: 4433–4453

Marchadier E, Hanemian M, Tisné S, Bach L, Bazakos C, Gilbault E, Haddadi P, Virlouvet L, Loudet O (2019) The complex genetic architecture of shoot growth natural variation in Arabidopsis thaliana. PLoS Genet 15: 1–27

McCormick AJ, Kruger NJ (2015) Lack of fructose 2,6-bisphosphate compromises photosynthesis and growth in Arabidopsis in fluctuating environments. Plant J 81: 670–683

Paul MJ, Foyer CH (2001) Sink regulation of photosynthesis. J--Exp-Bot 52: 1383–1400

Paul MJ, Pellny TK (2003) Carbon metabolite feedback regulation of leaf photosynthesis and development. J Exp Bot 54: 539–547

Petrík P, Petek-Petrik A, Mukarram M, Schuldt B, Lamarque LJ (2023) Leaf physiological and morphological constraints of water-use efficiency in C3 plants. AoB PLANTS 15: plad047

Preiser AL, Banerjee A, Weise SE, Renna L, Brandizzi F, Sharkey TD (2020) Phosphoglucoisomerase Is an Important Regulatory Enzyme in Partitioning Carbon out of the Calvin-Benson Cycle. Front Plant Sci 11: 580726

Ritchie M, Phipson B, Wu D, Hu Y, Law C, Shi W, Smyth G (2015) limma powers differential expression analysis for RNA-sequencing and microarray studies. Nucleic Acids Res 43: e47

Saddhe AA, Manuka R, Penna S (2021) Plant sugars: Homeostasis and transport under abiotic stress in plants. Physiol Plant 171: 739–755

Sehki H, Yu A, Elmayan T, Vaucheret H (2023) TYMV and TRV infect Arabidopsis thaliana by expressing weak suppressors of RNA silencing and inducing host RNASE THREE LIKE1. PLOS Pathog 19: e1010482

Slawinski L, Israel A, Artault C, Thibault F, Atanassova R, Laloi M, Dédaldéchamp F (2021) Responsiveness of Early Response to Dehydration Six-Like Transporter Genes to Water Deficit in Arabidopsis thaliana Leaves. Front Plant Sci 12: 1–21

Sorin C, Bussell JD, Camus I, Ljung K, Kowalczyk M, Geiss G, McKhann H, Garcion C, Vaucheret H, Sandberg G, Bellini C (2005) Auxin and light control of adventitious rooting in Arabidopsis require ARGONAUTE1. Plant Cell Online 17: 1343–1359

Stanfield RC, Bartlett MK (2022) Coordination Between Phloem Loading and Structure Maintains Carbon Transport Under Drought. Front Plant Sci 13:

Tcherkez G, Mahé A, Gauthier P, Mauve C, Gout E, Bligny R, Cornic G, Hodges M (2009) In Folio Respiratory Fluxomics Revealed by 13C Isotopic Labeling and H/D Isotope Effects Highlight the Noncyclic Nature of the Tricarboxylic Acid "Cycle" in Illuminated Leaves. Plant Physiol 151: 620–630

Tisné S, Serrand Y, Bach L, Gilbault E, Ben Ameur R, Balasse H, Voisin R, Bouchez D, Durand-Tardif M, Guerche P, Chareyron G, Da Rugna J, Camilleri C, Loudet O (2013) Phenoscope: An automated large-scale phenotyping platform offering high spatial homogeneity. Plant J 74: 534–544

Valifard M, Fernie AR, Kitashova A, Nägele T, Schröder R, Meinert M, Pommerrenig B, Mehner-Breitfeld D, Witte C-P, Brüser T, Keller I, Neuhaus HE (2023) The novel chloroplast glucose transporter pGlcT2 affects adaptation to extended light periods. J Biol Chem 299: 104741

Valifard M, Le Hir R, Müller J, Scheuring D, Neuhaus HE, Pommerrenig B (2021) Vacuolar fructose transporter SWEET17 is critical for root development and drought tolerance. Plant Physiol 187: 2716–2730

Vialet-Chabrand S, Matthews JSA, Brendel O, Blatt MR, Wang Y, Hills A, Griffiths H, Rogers S, Lawson T (2016) Modelling water use efficiency in a dynamic environment: An example using Arabidopsis thaliana. Plant Sci 251: 65–74

Weise SE, Liu T, Childs KL, Preiser AL, Katulski HM, Perrin-Porzondek C, Sharkey TD (2019) Transcriptional regulation of the glucose-6-phosphate/phosphate translocator 2 is related to carbon exchange across the chloroplast envelope. Front Plant Sci 10: 1–13

Wingenter K, Schulz A, Wormit A, Wic S, Trentmann O, Hoermiller II, Heyer AG, Marten I, Hedrich R, Neuhaus HE (2010) Increased activity of the vacuolar monosaccharide transporter TMT1 alters cellular sugar partitioning, sugar signaling, and seed yield in Arabidopsis. Plant Physiol 154: 665–677

Xu Q, Chen S, Yunjuan R, Chen S, Liesche J (2018) Regulation of Sucrose Transporters and Phloem Loading in Response to Environmental Cues. Plant Physiol 176: 930–945

Yamada K, Osakabe Y, Mizoi J, Nakashima K, Fujita Y, Shinozaki K, Yamaguchi-Shinozaki K (2010) Functional analysis of an Arabidopsis thaliana abiotic stress-inducible facilitated diffusion transporter for monosaccharides. J Biol Chem 285: 1138–1146

Zargar SM, Gupta N, Nazir M, Mahajan R, Malik FA, Sofi NR, Shikari AB, Salgotra RK (2017) Impact of drought on photosynthesis: Molecular perspective. Plant Gene 11: 154–159

Zhang Y, Fernie AR (2018) On the role of the tricarboxylic acid cycle in plant productivity. J Integr Plant Biol 60: 1199–1216

Supplementary data

Fig. S1. Rosette growth of *sweet* mutant lines grown under short-days photoperiod.

Fig. S2. Maximum rosette leaves temperature is impaired in *swt11swt12* mutant line.

Fig. S3. Expression of SWEET transporters in the rosette leaves grown under short-days photoperiod.

Fig. S4. Proline synthesis is upregulated in response to drought stress.

Fig. S5. Metabolites specifically accumulating or decreasing in response to different drought stress in wild type or *swt-q* mutant.

Table S1. Raw data of the metabolomic profiling.

Table S2. Primers used for quantifying genes by RT-qPCR.

Table S3. Metabolites significantly different in the different *sweet* mutant lines compared to wild-type plants grown in short-days photoperiod under normal watering conditions.

Table S4. Raw data of the *Phenoscope* experiment.

Table S5. Metabolites significantly different in wild-type plants grown in non-limiting conditions (60% SWC) or after the application of a long-term mild intensity stress (30% SWC).

Table S6. Metabolites significantly different in wild-type plants grown in non-limiting conditions (60% SWC) or after the application of a long-term medium intensity stress (25 % SWC).

Table S7. Metabolites significantly different in *swt-q* plants grown in non-limiting conditions (60% SWC) or after the application of a long-term mild intensity stress (30 % SWC).

Table S8. Metabolites significantly different in *swt-q* plants grown in non-limiting conditions (60% SWC) or after the application of a long-term medium intensity stress (25 % SWC).

Table S9. Metabolites significantly different between both genotypes and both drought stress conditions.

Table S10. Sugar response of genes significantly deregulated in *sweet* mutant lines.

Table 1. Log_2-fold changes of genes involved in sugar homeostasis in cytosol and chloroplast in *sweet* mutant plants compared to WT grown in short-days photoperiod.

Full rosettes have been harvested and used for mRNA extraction and subsequent qPCR experiment. Bold-scripted Log_2FC indicate significant fold changes ($p < 0.05$) while stars indicate Log_2FC values for which p is comprised between 0.05 and 0.09 according to a double-sided t test.

Gene description		Gene name	Gene number	Log_2FC *swt11swt12*/WT	Log_2FC *swt16swt17*/WT	Log_2FC *swt-q*/WT
Cytosolic glycolysis	Hexokinase	*HXK1*	At4g29130	-0.23	-0.03	0.04
	Phosphoglucoisomerase	*cPGI*	At5g42740	0.30	0.55	0.17
	Phosphofructokinase	*PFK1*	At4g29220	**0.21**	**0.32**	**0.31**
		PFK7	At5g56630	-0.07	-0.10	0.12
	Fructose-bisphosphate aldolase	*FBA4*	At5g03690	**-0.87**	-0.34*	0.02
		FBA5	At4g26530	0.10	**0.51**	-0.10
		FBA6	At2g36460	**-0.52**	-0.07	-0.04
		FBA7	At4g26520	**-2.86**	**-1.00**	**0.55**
		FBA8	At3g52930	-0.05	**0.21**	0.08
	Fructose-2,6-bisphosphatase	*F2KP*	At1g07110	**0.62**	**0.81**	0.27
	Fructose-1,6-bisphosphatase	*cyFBP/FINS1*	At1g43670	-0.19	0.04	0.02
Chloroplastic glycolysis	Hexokinase	*HXK3*	At1g47840	0.15	**0.36**	0.00
	Phosphoglucoisomerase	*pPGI*	At4g24620	0.39*	**0.63**	0.15
	Phosphofructokinase	*PFK5*	At2g22480	**0.48**	**0.56**	**0.38**
	Fructose-bisphosphate aldolase	*pFBA1*	At2g21330	0.15	0.30*	0.08
		pFBA2	At4g38970	0.16	**0.45**	-0.25
		pFBA3	At2g01140	0.22*	0.20*	0.02
	Fructose 1,6-bisphosphate phosphatase	*cFBP1/HCEF1*	At3g54050	0.08	0.16	0.07
Starch synthesis and degradation	AGPase small subunit	*ADG1/APS1*	At5g48300	**0.51**	**0.42**	**0.38**
	AGPase large subunit	*APL3*	At4g39210	0.18	0.12	0.16
		APL4	At2g21590	0.19	0.54	-0.36
	Beta-amylase	*BAM1*	At3g23920	-0.12	0.26*	-0.06
		BAM3	At4g17090	0.06	0.26	0.09
Tonoplastic sugar transporters	Fru exporter	*ERDL4/ESL1,01*	At1g19450	-0.12	0.08	-0.01
	Glc and fru exporter	*ESL1*	At1g75220	-0.39	-0.25	-0.07
	Sucrose exporter	*SUC4*	At1g09960	-0.22	-0.08	-0.21
	Glucose facilitator	*SWEET2*	At3g14770	-0.21	0.22	-0.20
	Glc and fru importer	*TST1/TMT1*	At1g20840	**-0.34**	-0.13	-0.24
	Glucose importer	*VGT1*	At3g03090	-0.05	0.28*	0.04
Plastid sugar transporters	Glc-6-P/P-Translocator	*GPT2*	At1g61800	**0.95**	0.52	**0.94**
	Maltose exporter	*MEX1*	At5g17520	-0.05	0.13	**0.31**
	plastid glc exporter	*pGlcT*	At5g16150	0.12	**0.33**	0.21
	Triose phosphate translocator	*TPT*	At5g46110	**-0.23**	-0.08	**-0.21**

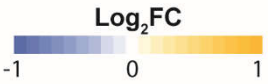

Table 2. Log_2-fold changes (FC) of genes involved in sugar homeostasis in cytosol and chloroplast in *swt-q* mutant plants and WT grown in mild intensity (30% SWC) or medium intensity (25% SWC) drought stress compared to normal watering conditions (60% SWC).

Full rosettes have been harvested and used for mRNA extraction and subsequent qPCR experiment. Bold-scripted Log_2FC indicate significant fold changes ($p < 0.05$) while stars indicate Log_2FC values for which *P* is comprised between 0.05 and 0.09 according to a double-sided *t* test. The results of GxE interaction from the two-way ANOVA is also displayed (* $p < 0.05$, ** $p < 0.01$, • $0.05 < p < 0.09$, NS: not significant).

Gene description		Gene name	Gene number	Log_2 FC WT 30% SWC/ WT 60% SWC	Log_2 FC WT 25% SWC/ WT 60% SWC	Log_2 FC swt-q 30% SWC/ swt-q 60% SWC	Log_2 FC swt-q 25% SWC/ swt-q 60% SWC	Interaction GxE
Stress markers	Low temperature responsive protein	*RD29a/COR78*	At5g52310	**1.59**	**1.46**	0.55	**1.73**	NS
	Delta1-pyrroline-5-carboxylate synthase	*P5CS2*	At3g55610	**0.60**	**0,46**	**0.28**	0.13	NS
	Tonoplastic sugar transporter	*ESL1*	At1g75220	0.34	0.11	**0.33**	**0.74**	NS
Photosynthesis markers	Rubisco small subunit	*RBCS3B*	At5g38410	0.18*	0.12	0.00	0.09	NS
	Light harvesting chlorophyll A/B-binding protein	*LHCB1.1/CAB2*	At1g29920	0.31	0.09	-0.02	-0.01	NS
		LHCB1.3/CAB1	At1g29930	0.16	0;28	-0.09	0.22	NS
Mitochondrial respiratory chain	Gamma carbonic anhydrase	*gammaCA1*	At1g19580	0.20	-0.23	0.05	**0.43**	* (p = 0,0367)
		gammaCA2	At1g47260	0.14	-0.03	0.01	0.16	NS
Cytosolic glycolysis	Phosphoglucoisomerase	*cPGI*	At5g42740	0.23	0.05	-0.10	0.00	NS
		FK2P	At1g07110	0.31	0.04	-0.03	-0.14	NS
	Fructokinase	*FRK2*	At2g31390	**-0.26**	-0.31	0.00	-0.06	NS
		FRK6	At1g06030	-0.28	-0.35	0.04	0.17	NS
		FRK7	At3g59480	-0.35	**-0.66**	**-0.55**	**-0.47**	NS
	Phosphofructokinase	*PFK1*	At4g29220	0.29*	0.17	0.02	0.14	NS
		PFK7	At5g56630	**0.19**	-0.02	0.05	0.12	NS
Chloroplastic glycolysis	Fructose 1,6-bisphosphate phosphatase	*cFBP1/HCEF1*	At3g54050	-0.38	-0.17	-0.06	0.19	NS
	Phosphoglucoisomerase	*pPGI*	At4g24620	0.35*	0.08	-0.14	-0.05	NS
	Phosphoglucomutase	*pPGM*	At5g51820	0.10	-0.04	-0.04	-0.02	NS
	Fructokinase	*FRK3*	At1g66430	0.31	0.24	**0.37**	**0.68**	• (p = 0,084)
	Hexokinase	*HXK3*	At1g47840	-0.08	-0.20	-0.12	-0.06	NS
	Phosphofructokinase	*PFK5*	At2g22480	0.34*	0.00	0.17	-0.01	NS
	Fructose 1,6-bisphosphate phosphatase	*cyFBP/FINS1*	At1g43670	0.07	0;10	0.03	0.15	NS
Starch synthesis and degradation	AGPase small subunit	*ADG1*	At5g48300	0.03	0.05	-0.10	-0.15	NS
	AGPase large subunit	*APL3*	At4g39210	0.14	0.16	0.37	**0.84**	• (p = 0,081)
		APL4	At2g21590	0.73	0.04	0.78	**1.30**	• (p = 0,056)
	Beta-amylase	*BAM1*	At3g23920	0.38	0.23	0.27	**0.84**	• (p = 0,063)
		BAM3	At4g17090	0.09	-0.29	-0.45	0.34	NS
Plastid sugar transporters	Glc-6-P/Pi translocator	*GPT2*	At1g61800	0.32	-0.51	-0.35	0.33	NS
	Plastid glucose transporter	*pGlcT*	At5g16150	0.26	0.17	0.16	-0.19	NS
	Maltose transporter	*MEX1*	At5g17520	**0.54**	**0.43**	**0.34**	**0.72**	** (p = 0,00937)

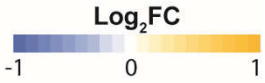

Figure legends

Fig. 1. Disruption of *SWEET11* and *SWEET12* leads to a loss of photosynthesis efficiency. effective quantum yield of PSII [Y(II)] (A), the electron transport rate (ETR) (B) and the quantum yield of non-photochemical quenching [Y(NPQ)] (C) were determined using a light curve of increasing PAR intensity performed on wild types, *swt11swt12*, *swt16swt17* and *swt-q* mutants. Values are means ± SE (n = 12 plants). Significant differences were calculated using a student's *t* test with * $p<0.05$ and • $0.05 < p < 0.09$.

Fig. 2. Assimilation and transpiration rates are impaired in *sweet* mutant lines. Barplots showing the stomatal conductance (A), the transpiration rate (B), the assimilation rate (C), the intracellular CO_2 concentration (C_i) (D), the ratio assimilation/transpiration or water use efficiency (WUE) (E) and assimilation/stomatal conductance or intrinsic water use efficiency (WUE_i) (F) of wild types, *swt11swt12*, *swt16swt17* and quadruple mutants grown in short-days photoperiod. Means ± SE are shown (n = 12 individual leaves per genotype coming from 6 plants). A one-way ANOVA combined with the Tukey's comparison post hoc test was performed. The values marked with the same letter were no significantly different from each other whereas different letters indicate significant differences ($p < 0.05$).

Fig. 3. Metabolites involved in sugar metabolism and Krebs cycle are accumulating in rosette leaves of *sweet* mutant lines. Heatmap of the changes in the metabolite contents in the *swt11swt12*, *swt16swt17* and *swt-q* mutant lines grown in the phenotyping robot. Values presented are Log_2 transformed mutant-to-wild-type ratio ($n \geq 7$ per genotype). The colour gradient from yellow to blue refers to metabolites accumulated or decreased, respectively, in the mutant lines compared to WT. Only metabolites displaying a statistical difference are shown as Log_2 fold-change. Values with $p < 0.05$ were considered significantly different. Additional stars in boxes indicate metabolites significantly different between *swt11swt12* and *swt-q* mutants. Crossed out boxes: metabolite showing no statistical differences. ND: not detected.

Fig. 4. Starch accumulates in rosette leaves of *sweet* mutant lines. Barplot showing the starch content of rosette leaves of wild type and *sweet* mutant lines grown in short-days photoperiod. Means ± SD are shown (n = 6 plants per genotype). A one-way ANOVA combined with the Tukey's comparison post hoc test was performed. The values marked with the same letter were no significantly different from each other whereas different letters indicate significant differences ($p < 0.05$).

Fig. 5. *swt-q* mutant line is more sensitive to drought stress. Barplots showing the fold-changes in the projected rosette area (A), the convex hull area (B) and the compactness (C) of wild type and quadruple mutant grown in short-days photoperiod under different watering regime: 60% SWC (normal watering conditions), 30 % SWC (mild stress intensity) or 25% SWC (medium stress intensity). The fold changes were determined using the values that were normalized to the mean of wild-type plants grown at 60% SWC. A two-way ANOVA combined with the Tukey's comparison post hoc test was performed. The values marked with the

same letter were no significantly different from each other whereas different letters indicate significant differences ($p < 0.05$, $n \geq 18$ per genotype and condition from 2 independent experiments).

Fig. 6. *swt-q* mutant accumulates more sugars than wild type in response to drought stress. Heat map of the changes in the metabolite contents in the wild-type plants and the *swt-q* mutant line grown in short-days photoperiod under different watering conditions. The orange to green gradient refers to metabolites accumulated (yellow) or decreased (blue) for both wild-type plants and *swt-q* mutant. The values presented in the two upper squares are Log_2 fold-change ratio of wild-type plants grown under 30% SCW (mild stress intensity) (left square) and 25% SWC (medium stress intensity) (right square) compared to WT grown under 60 % SWC (normal conditions). The values presented in the two lower squares are Log_2 fold-change ratio of *swt-q* plants grown under 30% SCW (mild stress intensity) (left square) and 25% SWC (medium stress intensity) (right square) compared to *swt-q* grown under 60 % SWC (normal conditions). Additional stars in boxes indicate metabolites significantly different between wild type and *swt-q* mutant. Only metabolites showing a significant difference according a One-way ANOVA followed by a Tukey HSD post-test are presented ($p < 0.05$, $n \geq 7$ plants per genotype and condition). Crossed out boxes: metabolite showing no statistical differences. ND: not detected.

Fig. 7. SWEET transporters are regulated at both transcriptional and translational levels in response to drought stress. Barplots showing the changes of expression of *SWEET11* (A), *SWEET12* (B), *SWEET16* (C) and *SWEET17* (D) in wild-type plants grown in the different watering conditions on the *Phenoscope*. Full rosettes have been harvested and used for mRNA extraction and subsequent qPCR experiment. Translational SWT-GUS fusions were also grown on the *Phenoscope* in the different water regimes and used to assess the GUS activity (E). Means ± SE are shown (n = 4 plants per condition). A student *t*-test was performed with * $p < 0.05$, ** $p < 0.01$ and *** $p < 0.001$. ND: not detected.

Fig. 8. Proposed model of the involvement of SWEET11 and SWEET17 in photosynthesis. Synthesis scheme in wild-type plants (A), *swt11swt12* (B), *swt16swt17* (C) and *swt-q* (D) mutant lines. Within the mesophyll and phloem parenchyma cells, the vacuole is presented in light grey, the chloroplasts in green, the mitochondria in yellow and a starch granule is depicted in purple. The light green double-headed arrow across the stomata in (B) refers to the potential increased in stomatal opening in the mutant lines. The differences in the colour intensity of the chloroplasts, mitochondria and starch granule represents changes in PSII efficiency, accumulation of organic acids and starch accumulation, respectively. Finally, the size of the character (CO_2, and H_2O) refers to the increase compared to wild-type plants. To avoid overloading the figure, the organites in the companion cell/sieve element complex are not presented. CC/SE: companion cells/sieve elements complex, Ep: epidermis, MCs: mesophyll cells, PP: phloem parenchyma cells.

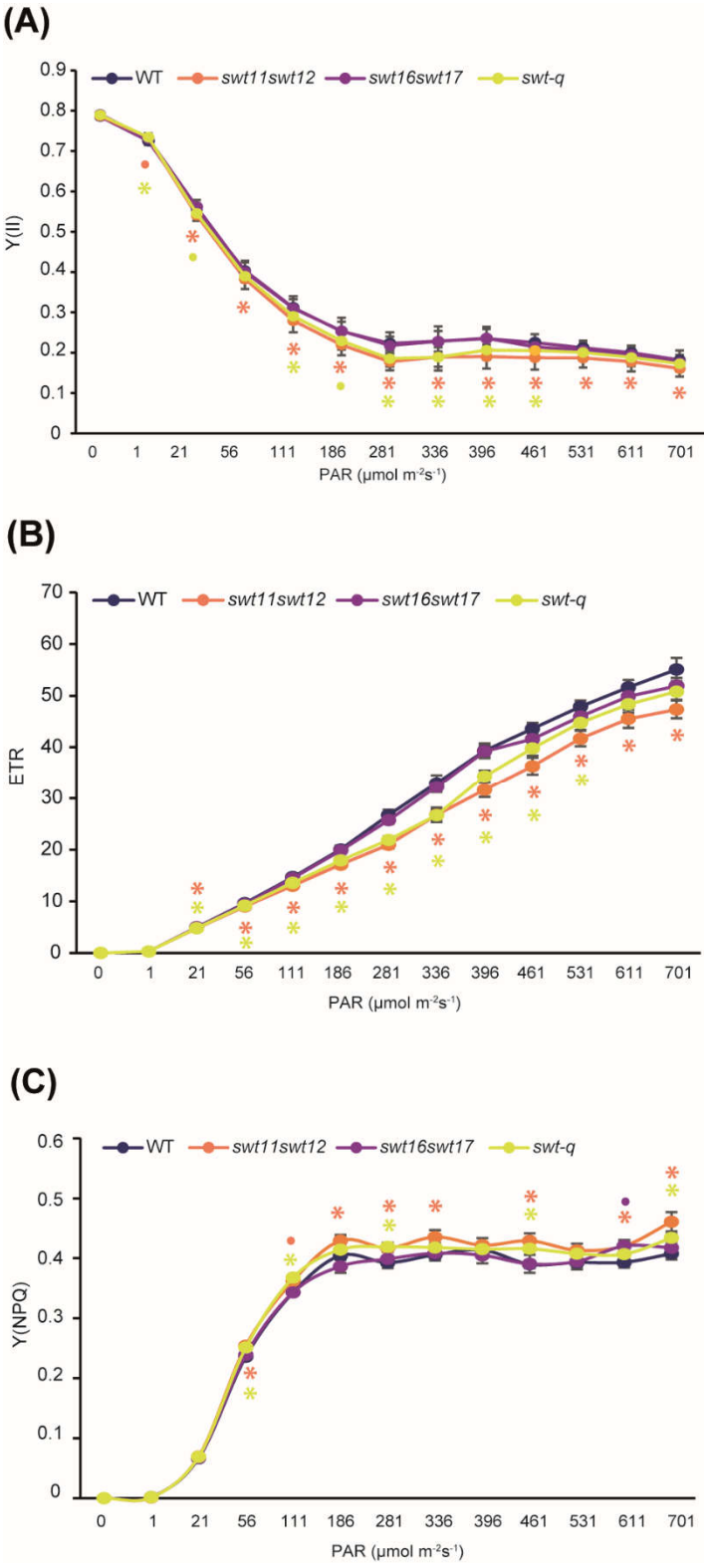

Fig. 1. Disruption of *SWEET11* and *SWEET12* leads to a loss of photosynthesis. effective quantum yield of PSII [Y(II)] (A), the electron transport rate (ETR) (B) and the quantum yield of non-photochemical quenching [Y(NPQ)] (C) were determined using a light curve of increasing PAR intensity performed on wild types, *swt11swt12*, *swt16swt17* and *swt-q* mutants. Values are means ± SE (n = 12 plants). Significant differences were calculated using a student's *t* test with * $p<0.05$ and • $0.05 < p < 0.09$.

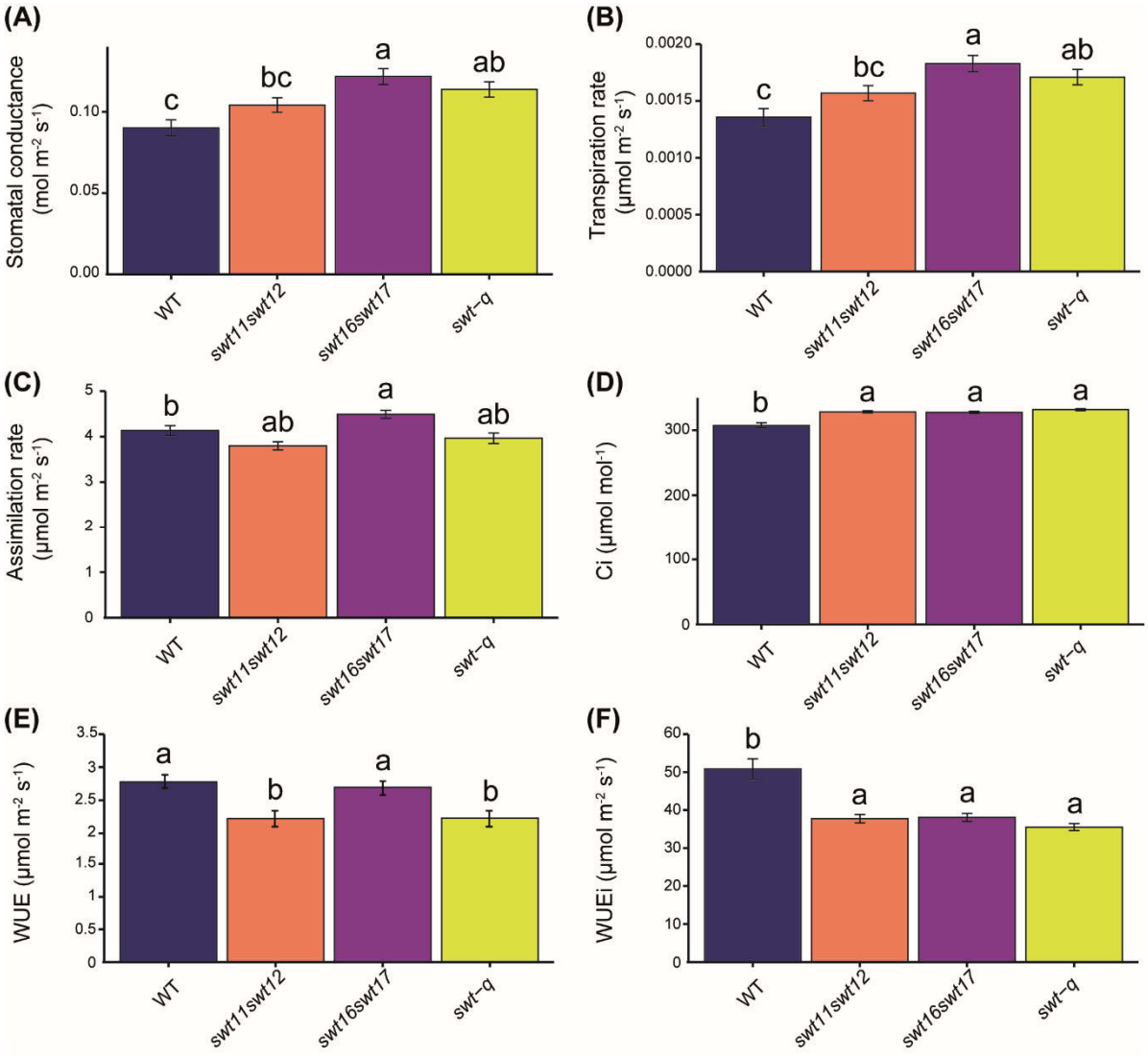

Fig. 2. Assimilation and transpiration rates are impaired in *sweet* mutant lines. Barplots showing the stomatal conductance (A), the transpiration rate (B), the assimilation rate (C), the intracellular CO_2 concentration (C_i) (D), the ratio assimilation/transpiration or water use efficiency (WUE) (E) and assimilation/stomatal conductance or intrinsic water use efficiency (WUE_i) (F) of wild types, *swt11swt12*, *swt16swt17* and quadruple mutants grown in short-days photoperiod. Means ± SE are shown (n = 12 individual leaves per genotype coming from 6 plants). A one-way ANOVA combined with the Tukey's comparison post hoc test was performed. The values marked with the same letter were no significantly different from each other whereas different letters indicate significant differences ($p < 0.05$).

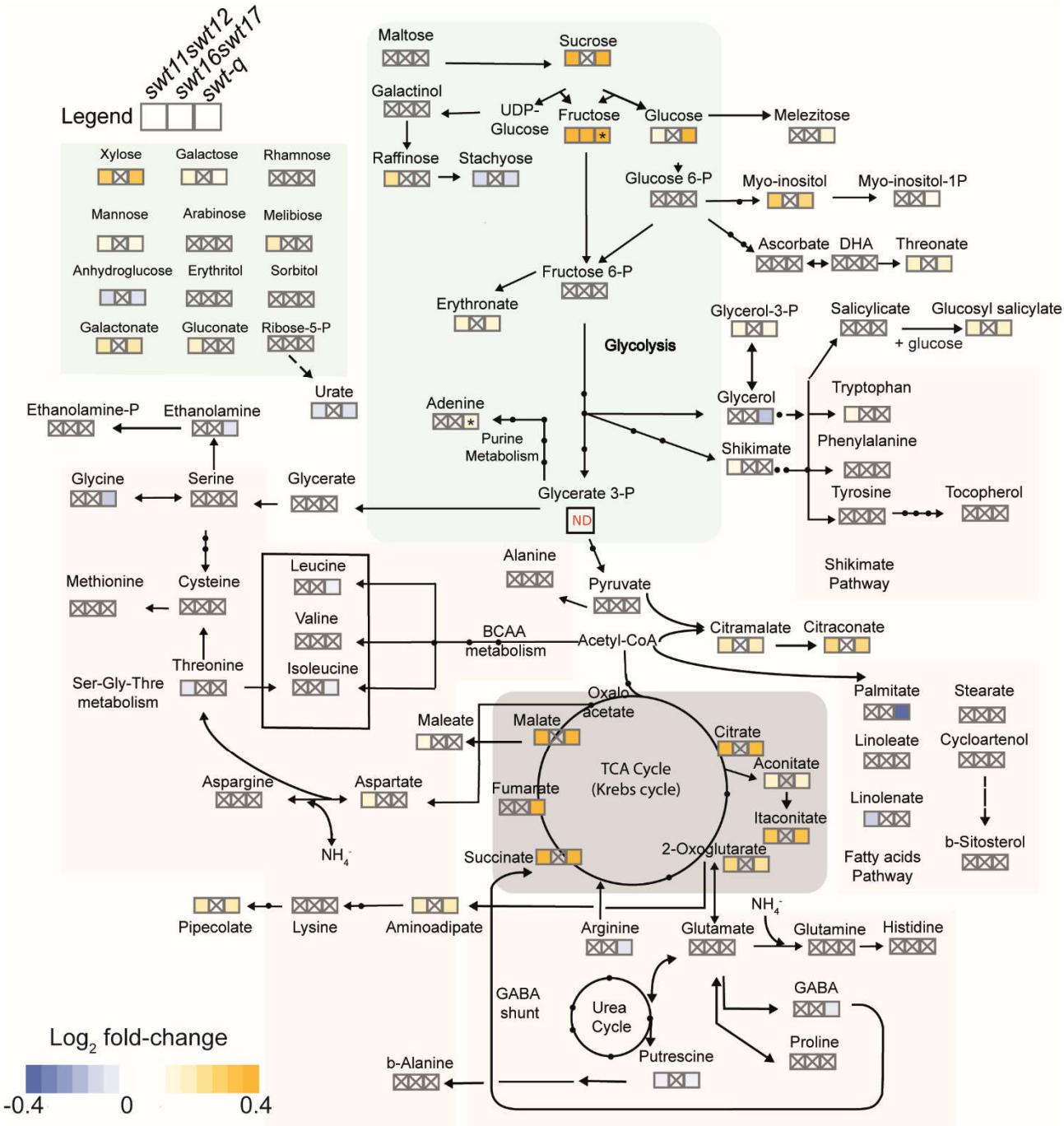

Fig. 3. Metabolites involved in sugar metabolism and Krebs cycle are accumulating in rosette leaves of *sweet* mutant lines. Heatmap of the changes in the metabolite contents in the *swt11swt12*, *swt16swt17* and *swt-q* mutant lines grown in the phenotyping robot. Values presented are Log_2 transformed mutant-to-wild-type ratio ($n \geq 7$ per genotype). The colour gradient from yellow to blue refers to metabolites accumulated or decreased, respectively, in the mutant lines compared to WT. Only metabolites displaying a statistical difference are shown as Log_2 fold-change. Values with $p < 0.05$ were considered significantly different. Additional stars in boxes indicate metabolites significantly different between *swt11swt12* and *swt-q* mutants. Crossed out boxes: metabolite showing no statistical differences. ND: not detected.

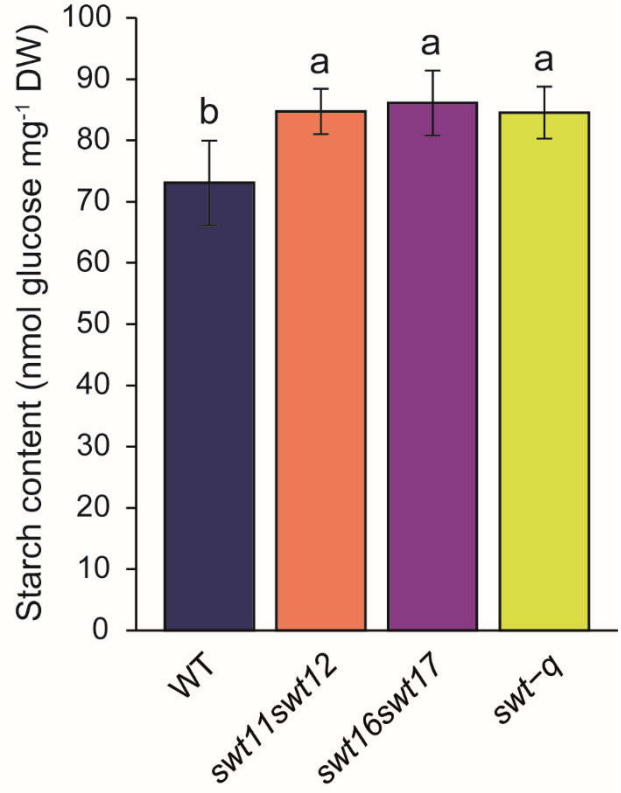

Fig. 4. Starch accumulates in rosette leaves of *sweet* mutant lines. Barplot showing the starch content of rosette leaves of wild type and *sweet* mutant lines grown in short-days photoperiod for 43 days. Means ± SD are shown (n = 6 plants per genotype). A one-way ANOVA combined with the Tukey's comparison post hoc test was performed. The values marked with the same letter were no significantly different from each other whereas different letters indicate significant differences ($p < 0.05$).

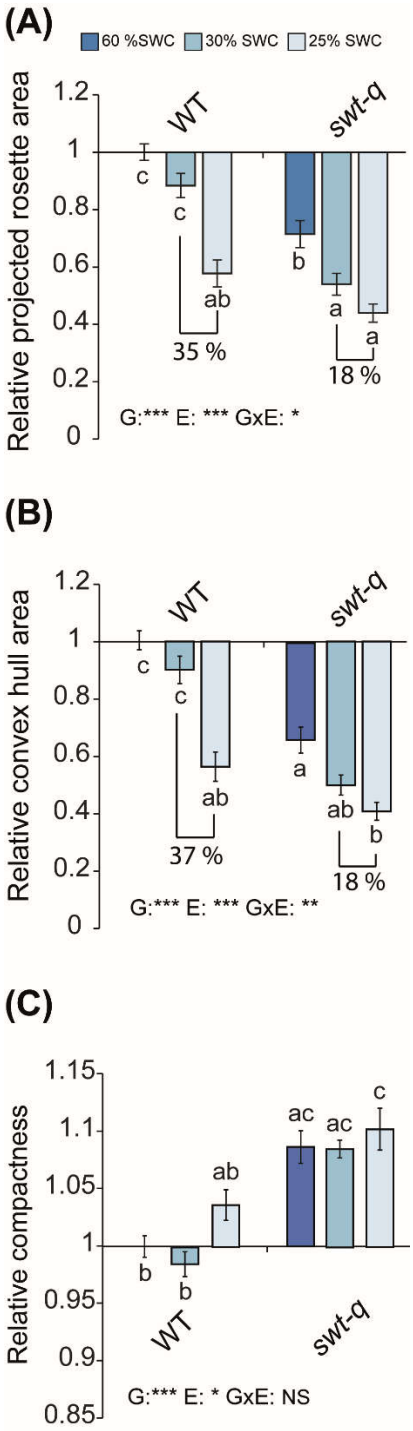

Fig. 5. *swt-q* mutant line is more sensitive to drought stress. Barplots showing the fold-changes in the projected rosette area (A), the convex hull area (B) and the compactness (C) of wild type and quadruple mutant grown in short-days photoperiod under different watering regime: 60% SWC (normal watering conditions), 30 % SWC (mild stress intensity) or 25% SWC (medium stress intensity). The fold changes were determined using the values that were normalized to the mean of wild-type plants grown at 60% SWC. A two-way ANOVA combined with the Tukey's comparison post hoc test was performed. The values marked with the same letter were no significantly different from each other whereas different letters indicate significant differences ($p < 0.05$, $n \geq 18$ per genotype and condition from 2 independent experiments).

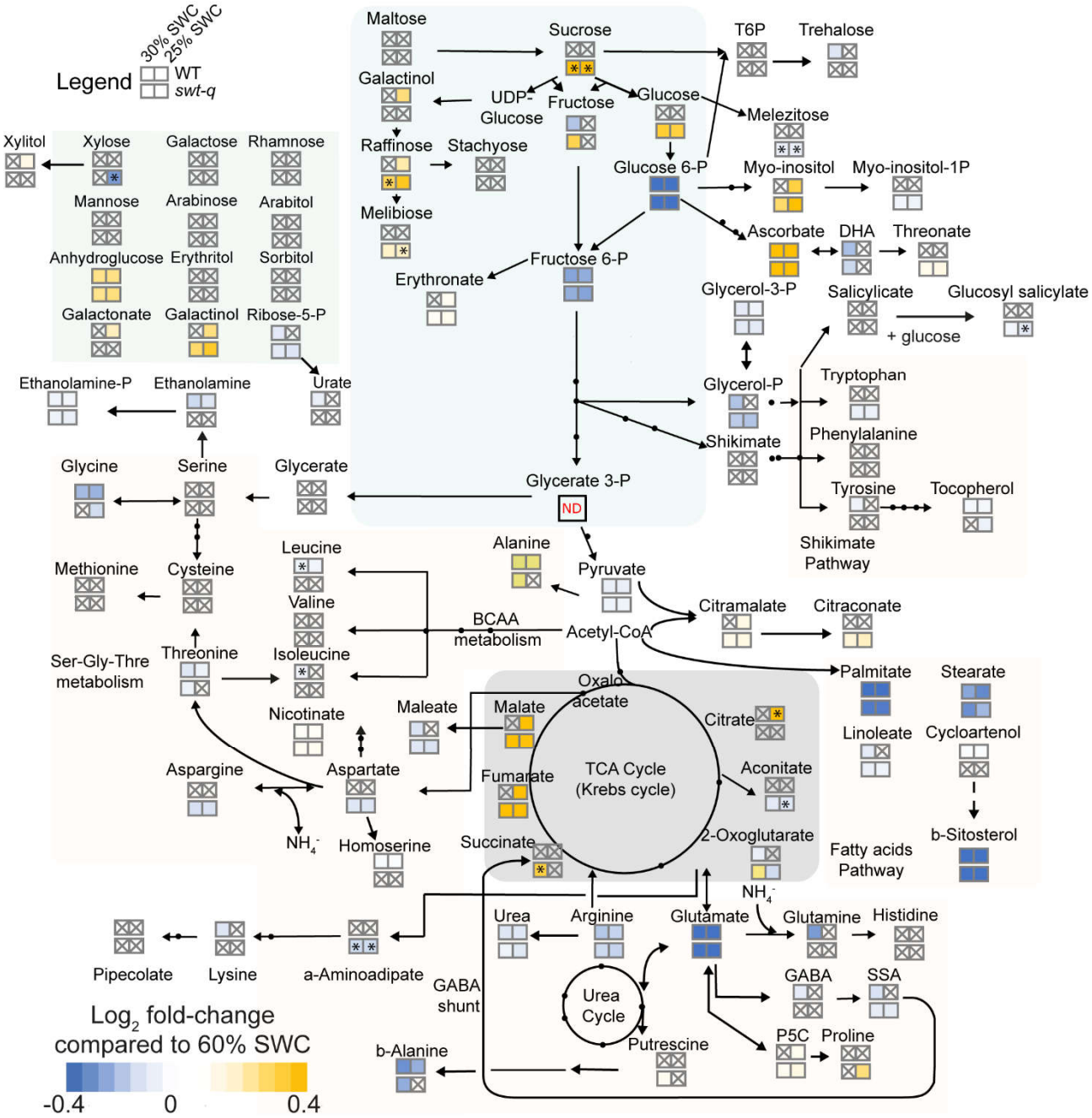

Fig. 6. *swt-q* mutant accumulates more sugars than wild type in response to drought stress. Heat map of the changes in the metabolite contents in the wild-type plants and the *swt-q* mutant line grown in short-days photoperiod under different watering conditions. The orange to green gradient refers to metabolites accumulated (yellow) or decreased (blue) for both wild-type plants and *swt-q* mutant. The values presented in the two upper squares are Log_2 fold-change ratio of wild-type plants grown under 30% SCW (mild stress intensity) (left square) and 25% SWC (medium stress intensity) (right square) compared to WT grown under 60 % SWC (normal conditions). The values presented in the two lower squares are Log_2 fold-change ratio of *swt-q* plants grown under 30% SCW (mild stress intensity) (left square) and 25% SWC (medium stress intensity) (right square) compared to *swt-q* grown under 60 % SWC (normal conditions). Additional stars in boxes indicate metabolites significantly different between wild type and *swt-q* mutant. Only metabolites

showing a significant difference according a One-way ANOVA followed by a Tukey HSD post-test are presented ($p < 0.05$, $n \geq 7$ plants per genotype and condition). Crossed out boxes: metabolite showing no statistical differences. ND: not detected.

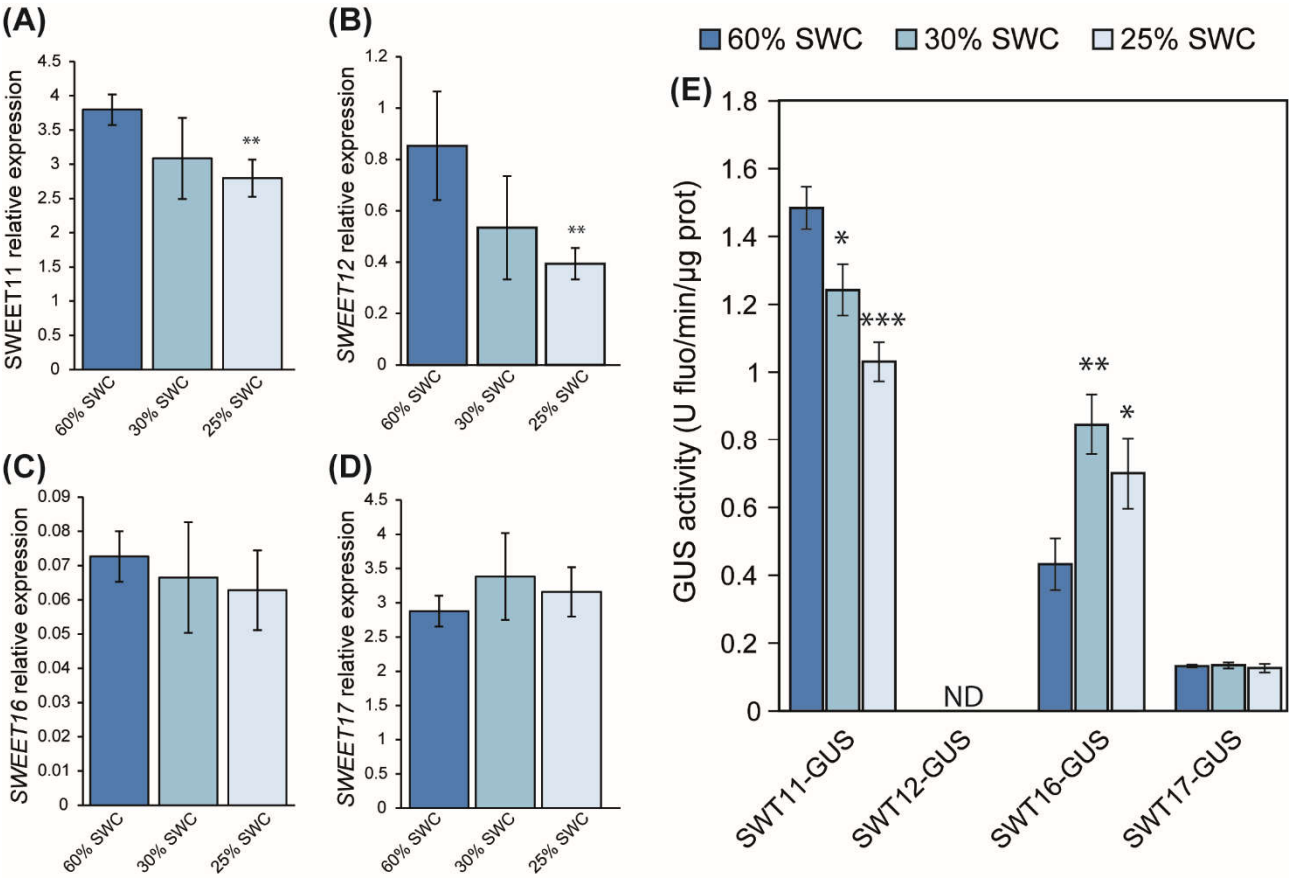

Fig.7. SWEET transporters are regulated at both transcriptional and translational levels in response to drought stress. Barplots showing the changes of expression of *SWEET11* (A), *SWEET12* (B), *SWEET16* (C) and *SWEET17* (D) in wild-type plants grown in the different watering conditions on the *Phenoscope*. Full rosettes have been harvested and used for mRNA extraction and subsequent qPCR experiment. Translational SWT-GUS fusions were also grown on the *Phenoscope* in the different water regimes and used to assess the GUS activity (E). Means ± SE are shown (n = 4 plants per condition). A student *t*-test was performed with * $p < 0.05$, ** $p < 0.01$ and *** $p < 0.001$. ND: not detected.

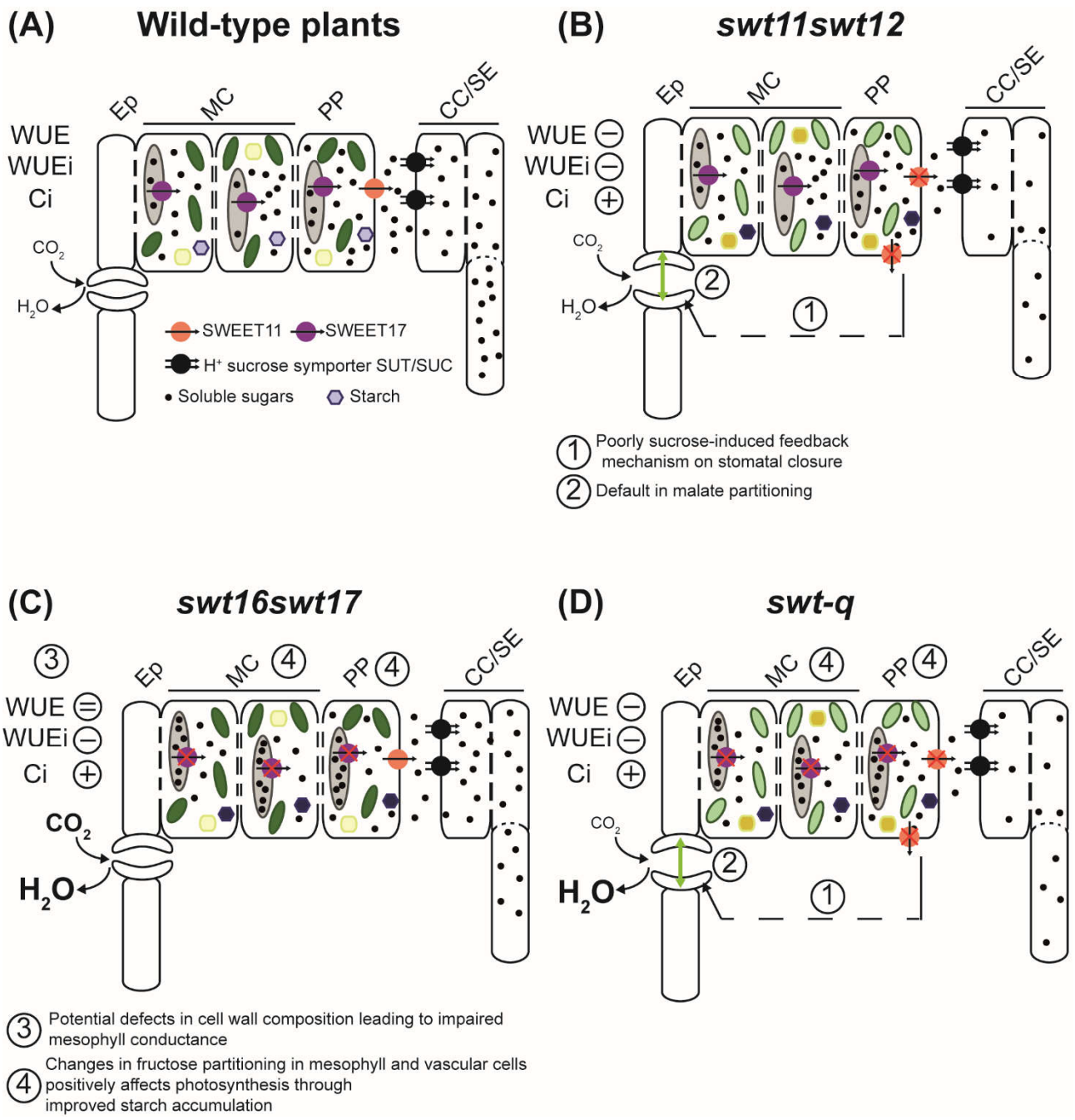

Fig. 8. Proposed model of the involvement of SWEET11 and SWEET17 in photosynthesis. Synthesis scheme in wild-type plants (A), *swt11swt12* (B), *swt16swt17* (C) and *swt-q* (D) mutant lines. Within the mesophyll and phloem parenchyma cells, the vacuole is presented in light grey, the chloroplasts in green, the mitochondria in yellow and a starch granule is depicted in purple. The light green double-headed arrow across the stomata in (B) refers to the potential increased in stomatal opening in the mutant lines. The differences in the colour intensity of the chloroplasts, mitochondria and starch granule represents changes in PSII efficiency, accumulation of organic acids and starch accumulation, respectively. Finally, the size of the character (CO_2, and H_2O) refers to the increase compared to wild-type plants. To avoid overloading the figure, the organites in the companion cell/sieve element complex are not presented. CC/SE: companion cells/sieve elements complex, Ep: epidermis, MCs: mesophyll cells, PP: phloem parenchyma cells.